# 9. Source Contributions Assessment

This section addresses the principal goal of Project MOHAVE, to estimate the contribution of the Mohave Power Project (MPP) to visibility impairment in Grand Canyon National Park (GCNP). To a lesser extent this section addresses the contributions of other sources. While most of the discussion is concerned with the new data and assessments generated as a part of Project MOHAVE, historic and climatological assessments are used to provide a context from which to the evaluate the merits of the newer information.

## 9.1 What is the *a priori* basis for believing that MPP could be an important source of haze at GCNP?

A few simple elements in a logical argument provide the basis for suspecting that MPP may be contributing to visibility impairment at GCNP. As indicated in Section 6, particulate sulfate is one of the important components responsible for visibility impairment (14-18% of the light extinction). MPP and the Navajo Generating Station (NGS), located on the Colorado River to the southwest and east of GCNP respectively, are responsible for most of the $SO_2$ emissions in the region. At 40,325 tons/year and 76,219 tons/year respectively their emissions have corresponded to about 40% of the total point source $SO_2$ emissions within California, Arizona, and Nevada (Grand Canyon Visibility Transport Commission, 1996). $SO_2$ converted to sulfate particles in the atmosphere is responsible for the vast majority of ambient particulate sulfate.

Previous studies (Malm et al., 1989b; Richards et al., 1991) demonstrated that NGS was responsible for some of the haze in GCNP under certain meteorological conditions that occur in the winter. These involve drainage flow from NGS toward GCNP, usually with low clouds in the canyons. The clouds are thought to be responsible for more rapid conversion of $SO_2$ to particulate sulfate, which can produce occasionally dense hazes in the canyons.

Conditions that could result in MPP contributions to visibility impairment at GCNP involve flow from the southwest and either slow net transport speed or clouds to increase amount of particulate sulfate produced by conversion of the MPP emitted $SO_2$. As shown in Figure 7-7, we know that MPP emissions are usually transported towards the western end of GCNP by wind flow from the south in the summer (April through September) and away from GCNP by flow from the north in the winter (November through February). Though infrequent and short-lived, winter storm systems occasionally result in flow to the north or northeast with clouds present. While the early summer period is typically characterized by few clouds, from about mid-July through mid-September monsoon conditions bring moisture from the Gulf of California and Gulf of Mexico that results in frequent cumulus cloud formation during the daylight hours.

Project MOHAVE summer and winter intensive periods were chosen to coincide with periods that include the summer monsoon and winter storm conditions in order to investigate the wind pattern and cloud conditions that are thought to have the greatest chance for MPP contributions to haze at GCNP. Wind data and model results using CALPUFF indicate that for other seasons, MPP emissions are transported toward Meadview at a frequency between that observed for the summer and winter study periods.

These meteorological patterns also cause flow of emissions towards GCNP from source areas to the southwest in the summer, such as Southern California, northern Mexico, and the San Joaquin Valley and from sources such as NGS to the northeast during typical winter conditions. During the summer, the persistent flow from the south and southwest may result in MPP emissions becoming embedded in the emission plumes from the substantial upwind source areas, confounding the separate assessment of MPP impacts.

### 9.2 What do pre-Project MOHAVE assessments indicate about source contributions to visibility impairment at GCNP?

The 1979 VISTTA study provided early indications of transport to the Grand Canyon area from Southern California. Macias et al. (1981) analyzed a late June haze episode by collating information from intensive aerosol measurements at the eastern end of the Grand Canyon with routine monitoring at locations upwind and with calculated back-trajectories. They found that emissions had been rapidly transported into the desert after several days of stagnation and buildup over Southern California. An interesting feature of this smog front was a marked increase in the size (and hence scattering efficiency) of sulfate-containing particles.

The VISTTA case study was given a climatological context in studies by the National Park Service. Iyer et al. (1987) calculated daily back-trajectories for Hopi Point, in order to study routinely monitored sulfate concentrations there as a function of the arriving air's history. Statistical analyses associated from 14% to 26% of the observed sulfate in the individual years 1979-1984 with Southern California, from 7% to 24% with copper smelters in Ely Nevada and southeastern Arizona, and from 0% to 20% with MPP. (Note that the $SO_2$ emission rates have changed considerably since this period.) In a subsequent reanalysis of aerosol and meteorological data from the 1980's, Malm (1992) associates 27% of the observed sulfate to Southern California and Baja California, 14% to Arizona copper smelters, and 17% to MPP.

Soon after the VISTTA study, exploratory measurements had provided a chemical fingerprint for anthropogenic influence, showing an episode of increased ozone and light scattering at Spirit Mountain to coincide with a pulse of methyl chloroform and Freon-11 (Hoffer et al., 1981). Routine monitoring of halocarbons was initiated at Spirit Mountain and Meadview in the mid-1980's, along with other air quality measurements. Intensive sampling in and around Los Angeles (Bastable et al., 1990), and the Toxic Release Inventory of methylchloroform (Sheiman et al., 1990), showed the Los Angeles basin to be the main identifiable source area for regional halocarbons.

The urban California origin of the methylchloroform arriving at the Grand Canyon was confirmed by time series and trajectory analyses. These showed a clear weekday-weekend cycle in ambient concentrations, lagging the pattern of industrial emissions by the day or two needed to traverse the intervening desert (White et al., 1990). Nearly all above-background concentrations came in air that had passed near Los Angeles (Vasconcelos et al., 1996; Vasconcelos, 1998).

Hourly ozone concentrations, which were monitored only at Spirit Mountain, were observed to track concurrent methylchloroform concentrations and foregoing Los Angeles Basin ozone concentrations (White et al., 1991). On this empirical basis, most of the above-background ozone at Spirit Mountain was related to transport from urban Southern California. Hourly

scattering coefficients tracked hourly methylchloroform concentrations (Miller et al., 1990), but haze/methylchloroform ratios varied significantly from day to day, precluding a quantitative apportionment.

MPP is almost exactly on a line from the Los Angeles Basin to the Grand Canyon, so the same winds that carry MPP's emissions toward GCNP also bring air from Southern California. Air arriving at the canyon from MPP can thus be expected to have higher than average background sulfate concentrations, due to the apparent prominence of Southern California as a regional source. Conversely, air arriving at the GCNP from most other directions can be expected to have lower than average backgrounds. Consequently, receptor analyses based on natural atmospheric variability have great difficulty resolving the two sources' contributions. It appears likely, for example, that the large year-to-year variability (from 0% to 20%) in the Iyer et al. (1987) MPP attributions reflects instabilities in their apportionment of southwestern emissions between MPP and upwind industry.

The geographically induced collinearity between Southern California's and MPP's contributions can be sidestepped by focusing on emissions rather than transport as the source of the signal sought at Grand Canyon. Unscheduled hiatuses in MPP's operation sometimes cause emissions reductions that are unrelated to atmospheric transport, dispersion, and transformation. Outages can thus be viewed as unplanned experiments to test the actual ambient effect of reducing emissions.

In particular, MPP was inoperable for the seven-month period June through December, 1985. The effect of this outage was examined by Murray et al. (1990), using 1984-1987 SCENES data from Spirit Mountain, Meadview, and Hopi Point. The authors found interannual variabilities of 15%-25% in ambient sulfate levels, with data from the 1985 shutdown falling in the range for normal operation. No effect of the shutdown on the distribution of 24-hour sulfate concentrations was found, even after adjusting for meteorological variations with multiple regression analyses. The 95% confidence bounds for average MPP summer impact were from less than 11.6% to less than 21% at Meadview and less than 3.3% to 7.8% at Hopi Point during favorable transport conditions.

Switzer et al. (1996) revisited the 1985-1987 SCENES data from the perspective of daily plant operating levels, accounting in their analysis for numerous shorter outages in one or the other of MPP's two units. Like Murray et al. (1990), they could find no discernible change in the frequency distribution of Meadview particle sulfur levels during periods of partial or complete MPP shutdowns.

The empirical studies of ambient concentration as a function of plant load provide a kind of "ground truth" on the effect of reduced MPP emissions. Even their truths rest on assumptions, however. Murray et al. (1990) assume that MPP's emissions were the major relevant variable that changed during the 7-month plant shutdown, that emissions from other sources were the same as in surrounding years, and they only accounted for some aspects of meteorological variability. Switzer et al. (1996) assume that atmospheric transport is independent of plant operation, neglecting any possible effect of reduced loads on plume rise. They further assume that the Spirit Mountain observatory receives negligible MPP sulfate, an assumption that is

consistent with the findings of Murray et al., but that operational difficulties prevented Project MOHAVE from checking.

An instrumented aircraft was employed during several summers to map the emissions plume as far downwind of MPP as it could be followed (Hegg et al., 1985). These efforts focused on the morning hours, before the plume was entrained and diluted by the deepening surface mixing layer. The elevated plume was sufficiently coherent at this time to be detectable, by instrumentation, out to ranges in excess of 100 km. At extreme range, the plume was generally situated west of Lake Mead. In the afternoons, when winds were expected to carry emissions toward GCNP, extended tracking beyond a few kilometers proved impossible. Under these conditions MPP emissions were diluted to the point where they could not be distinguished in real time from the varying ambient background.

The Winter Haze Winter Haze Intensive Tracer Experiment (WHITEX) was designed to evaluate the feasibility of attributing single point source emissions to visibility impairment in selected geographical regions. WHITEX measurements were conducted during a six week period in January and February 1987. During this time, an artificial tracer, deuterated methane ($CD_4$), was released from the NGS at Page, AZ near the eastern end of the Grand Canyon. Aerosol, optical, tracer, and other properties were measured at Hopi Point, which is in GCNP, and other locations. Synoptic weather maps indicated a high frequency of high pressure over the area, which resulted in transport of the NGS plume from the northeast toward GCNP. Trajectory analysis and deterministic modeling indicated transport from the area of NGS to Hopi Point during the period with highest sulfate concentrations there.

The extinction budget at Hopi Point on the south rim of the Grand Canyon indicated that sulfate aerosol (and associated water) contributed two-thirds of the non-Rayleigh light extinction during WHITEX. Attribution analysis used the Tracer Mass Balance Regression (TMBR) receptor model and the Differential Mass Balance (DMB) hybrid model. The separate analyses estimated that NGS was responsible for 70% to 80% of the sulfates measured at Hopi Point during WHITEX (Malm et al., 1989b and Latimer et al., 1989). Based on these results, the NPS concluded that NGS contributed substantially to sulfate and light extinction at Hopi Point.

The WHITEX data analysis methodology, results, and use of the results were cause for considerable controversy. The National Academy of Sciences Committee on Haze in National Parks and Wilderness Areas evaluated WHITEX (National Research Council, 1990). The Committee neither fully supported or discredited the WHITEX report. Based on evaluations of meteorological, photographic, chemical, and other physical evidence, the Committee concluded "at some times during the study period, NGS contributed significantly to haze in CGNP." However, the committee also concluded that "WHITEX did not quantitatively determine the fraction of sulfate aerosol and resultant haze in GCNP that is attributable to NGS emissions."

A key uncertainty identified by the Committee is the use of TMBR and DMB to apportion secondary species such as sulfate. Limitations of the regression analysis noted by the committee are: "(1) satisfactory tracers were not available for all major sources; (2) the interpretation did not adequately account for the possible covariance between NGS contributions and those from other coal fired power plants in the region; and (3) both models employ an inadequate treatment of sulfur conversion, which is an important controlling factor in the formation of haze at GCNP."

Another limitation noted by the committee was the lack of measurements within the canyon (beneath the rim).

The NGS Visibility Study was conducted by the Salt River Project (SRP), the operators of NGS, with measurements from January 10 through March 31, 1990. Its purpose was to address visibility impairment in GCNP during the winter months and the levels of improvement that might be achieved if $SO_2$ emissions from NGS were reduced. The study was performed to provide input to the rulemaking process of the EPA regarding NGS $SO_2$ controls (Richards et al., 1991).

Perfluorocarbon tracers (PFT) were released from each of the three stacks of NGS. Surface and upper air meteorology, particle and gaseous components, and tracer were measured at many sites. Deterministic modeling was done to estimate the contribution of NGS and other sources to sulfate levels for two 6 day periods with poor visibility. Various data analysis techniques were used to examine the relationships among NGS emissions, meteorology, air quality, and visibility during both episode and non-episode conditions.

The SRP study concluded that NGS emissions were absent from the vicinity of Hopi Point most of the time. The study estimated that the average contribution of NGS to fine sulfur at Hopi Point was small, although NGS sulfur dominated during one 4-hour period. However, it was noted that the frequency of wind directions transporting the plume toward GCNP was lower than normal during this time period.

The contribution of soil dust to haze was the focus of intensive measurements in the final year of the SCENES program (White et al., 1994). Intercomparisons of the collocated and size resolved optical and aerosol measurements indicated that predominantly coarse-particle dusts contributed almost half of the total particle scattering at Meadview on spring and summer afternoons. Subsequent analyses of back-trajectories associated elevated dust concentrations with air from Southern California (Vasconcelos et al., 1996).

## 9.3 What can we learn about source contributions directly from the Project MOHAVE data?

Insight into the relative contributions to Grand Canyon sulfate by various source regions and categories has been provided by two analyses of spatial patterns of sulfate concentrations, modified CMB receptor modeling, and by analysis of the behavior of the PFT tracers released during Project MOHAVE and of other air mass tracers, such as methylchloroform. The findings of these analyses are discussed here.

### 9.3.1 Spatial Pattern Analyses

Gebhart and Malm (1997) and Henry (1997b) analyzed spatial patterns of sulfate in the Project MOHAVE region. Gebhart and Malm used empirical orthogonal function (EOF) analysis, a form of spatial factor analysis. They deduced four spatial patterns that together explained 82% of the particulate sulfur variance during the summer intensive. In order of decreasing importance, these EOF patterns encompassed sources along (1) the lower Colorado River Valley, including MPP and Las Vegas urban area; (2) the southern California urban area stretching toward northern Arizona and southern Nevada; (3) areas to the south of the study region, including northern Mexico; and (4) a California EOF addressing such areas as the San Joaquin Valley.

Henry (1997b), using the RMAPS technique described in Section 8.2, similarly identified summertime spatial patterns that included a southern California urban area gradient; a lower Colorado River Valley source including the MPP and the Las Vegas urban area; and a southeast area including southern Arizona and northern Mexico. Henry attributed about half of the sulfate observed at the western end of the GCNP to the lower Colorado River Valley area while at the central portion of the Canyon, the majority of the sulfate emanated from sources to the southeast. (Section 8.2 discusses how these findings compare with the observed patterns of the PFT tracer.)

White (1997b) critiqued the work of Henry and concluded that the lower Colorado River Valley spatial pattern might be merely an extension of the southern California urban area region. Nevertheless, both these investigators agree that summer GCNP sulfate and resulting haze emanates from several source regions probably stretching from southern California eastward through Arizona and northern Mexico.

### 9.3.2 Modified CMB Attributions

As part of Project MOHAVE, the CMB hybrid model, MCMB (described in Section 8.3.5) was used to identify the important area and point sources impacting the GCNP (Eatough *et al.*, 1999 – enclosed in Appendix C). Some eight area sources and four point sources were characterized by emissions profiles. Attributions of both $SO_2$ and sulfate due to each source were produced for both Meadview and the central portion of the GCNP.

According to this model, at Meadview, the MPP is responsible on average during the summer for about 40% of the $SO_2$, but only about 5% of the sulfate. Although MPP is the dominant $SO_2$ source in the region, a generally low conversion rate of $SO_2$ to sulfate means that it contributes a much smaller fraction of the sulfate. The most important sulfate contributor at Meadview was found to be the Las Vegas urban area. Other important contributors to sulfate at Meadview are sources to the west and southwest.

At the heart of the GCNP, the dominant source of sulfate was found to be emissions from Baja California, a conclusion that is similar to the modeled findings of the Grand Canyon Visibility Transport Commission (Grand Canyon Visibility Transport Commission, 1996). Las Vegas is still an important source, along with the San Joaquin Valley. There is also some suggestion that sources to the south and southeast are more important here than they were at the western end of the GCNP at Meadview.

### 9.3.3 Perfluorocarbon and Halocarbon Tracer Analyses

The perfluorocarbon tracers (PFTs) released from MPP and several other locations and measured at about 30 receptors provide a direct ability to identify flow patterns and the extent of dispersion during the intensives. Details of the releases and sampling are given in Section 7.2.3 and 7.2.4. Based on analysis of these measurements, the following description of the flow patterns emerges.

During the winter, the predominant flow feature is drainage down the Colorado River along lower terrain. Under these circumstances the dispersion is retarded by confinement within the terrain as reflected in relatively high average tracer concentrations at large downwind distances.

Sources on the Colorado River east of GCNP (e.g., NGS), as represented by the Dangling Rope tracer, can have significant influence throughout the entire length of the Grand Canyon and beyond. The MPP emissions in the winter were transported primarily to the south along the Colorado River and were soon beyond the few tracer monitoring sites to the south of MPP. The MPP tracer was above background levels for about 6% of 24-hour sample periods at Meadview and was never measured above background levels at Hopi Point during the winter intensive monitoring period.

Large site-maximum concentrations for the MPP tracer at the Las Vegas Wash and Overton Beach sites during winter demonstrate that dispersion during occasional transport in a direction opposite to the predominant flow is comparable to that in flow in the predominant direction. This is somewhat surprising since the principal mechanism for such contrary flow is the passage of synoptic weather systems that generally entail mixing through a much greater depth, implying significantly increased dispersion.

Summer flow is generally from the south along the Colorado River (El Centro and MPP tracers) and from the west or possibly the southwest from the western edge of the Mojave Desert (Tehachapi Pass tracer). The MPP tracer was found to be above background levels for more than 90% of the summer intensive monitoring days for the sites around Lake Mead (Meadview, Overton Beach, and Las Vegas Wash), north and northeast of MPP. At Hopi Point, the MPP tracer concentrations were measured above background levels for about half of the days during the summer.

There appears to be a convergence zone over much of the Mojave Desert because tracers from both of the California release locations (Tehachapi and El Centro) were above background in 20% to 30% of the 24-hour sample periods at all of the eastern Mojave Desert sites. Given that flows from the greater Los Angeles and San Diego/Tijuana urban areas are likely to be located between the paths taken by the tracers from these California release locations, emissions from these areas must be at least as frequently transported through this region. From this it is reasonable to conclude that the eastern Mojave Desert is a major transport route for emissions from much of the State of California during the summer.

Transient haze events near the mouth of the Grand Canyon might potentially be attributed to patches of effluent from MPP. However, project analysts found no pattern of association between measured MPP tracer concentrations and light scattering at Meadview for 12-hour averaging periods during the entire summer intensive monitoring period, or for 1-hour averaging periods during the time with continuous tracer measurements at Meadview. This finding is demonstrated in the scatter plots provided below in Figure 9-1 and Figure 9-2. Correlation coefficients for these data are virtually zero indicating an absence of overall stable proportionality between light scattering and tracer concentrations at Meadview. The absence of any obvious relationship cannot rule out MPP contributions to haze in the GCNP, but strongly suggests that other sources were primarily responsible for the haze.

Although hourly extinction was not associated with MPP tracer, it did track concentrations of methylchloroform and water vapor (tracers of opportunity for air from Southern California and southern Arizona/northern Mexico) at times during the summer intensive study, according to the Tracer Regression method of White et al. (1998) (see Section 8.3.3). Multiple linear regression

of extinction on MPP tracer, methylchloroform, and water vapor during a 14 day period accounted for 74% of the observed variance, with methylchloroform and water vapor the significant explanatory variables. From methylchloroform ans water vapor alone, one can predict the observed extinction within 10% (one deciview) almost two thirds of the time, 250 of 398 hours (see Figure 9-3). From the data in that figure, one can determine that observed extinction was within one deciview (dv) of the prediction from methylchloroform and water vapor almost two-thirds of the time, 250 of 398 hours. The residual, representing extinction decoupled from the regional methylchloroform and water vapor tracers, exhibited no evident relationship with the MPP tracer.

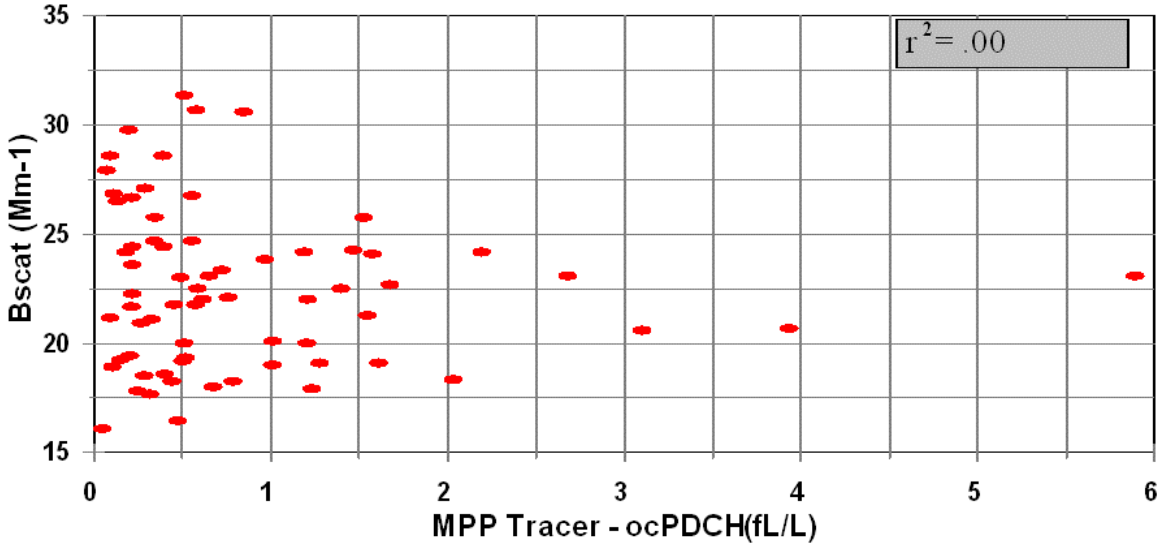


*Figure 9-1 Scatter plot of light scattering and MPP tracer at Meadview - 12 hour averaging time.*

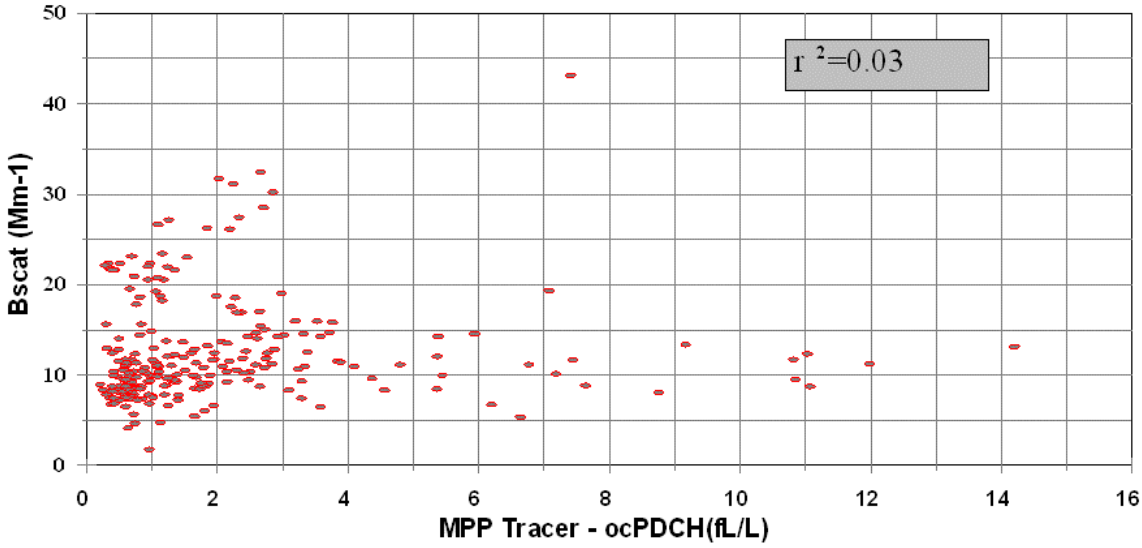


*Figure 9-2 Scatter plot of light scattering and MPP tracer at Meadview - 1 hour averaging time.*

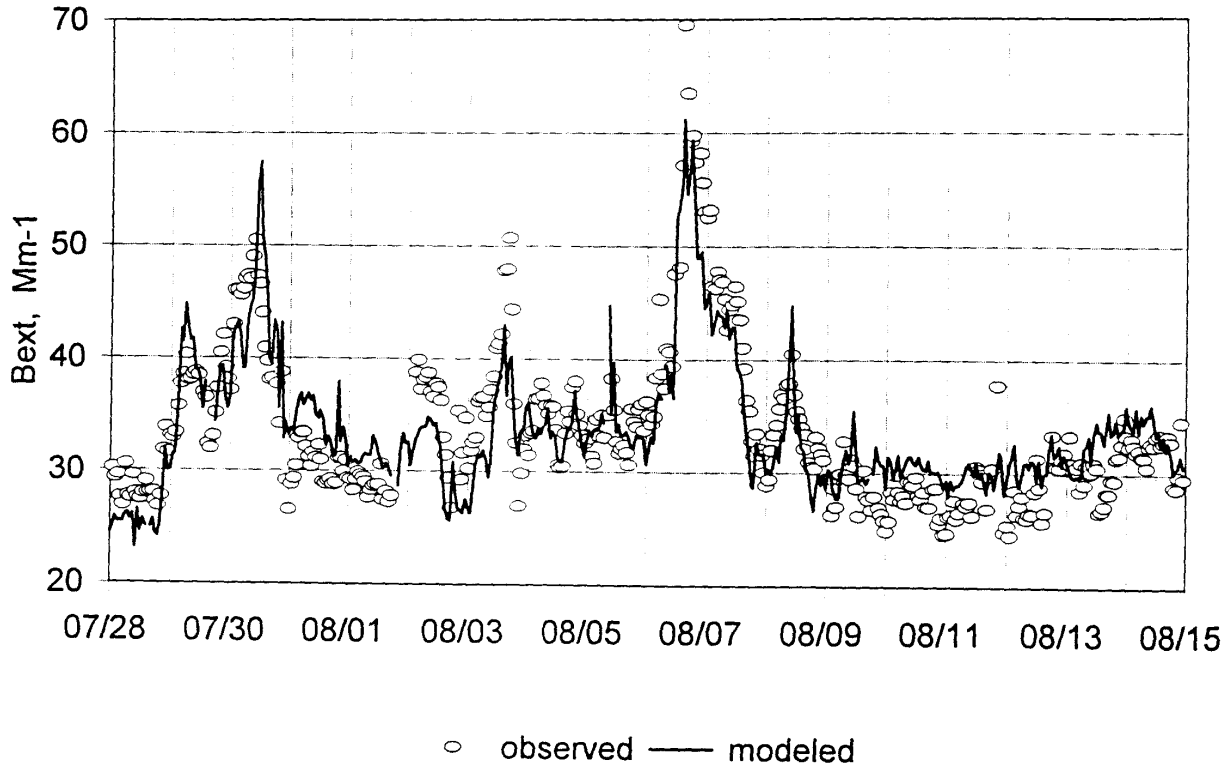


*Figure 9-3 Time series of measured light extinction and modeled light extinction as a linear function of methylchloroform and water vapor concentration.*

Two conclusions emerge fairly directly from these observations of PFT and halocarbons.

- Regional haze near the Grand Canyon can exhibit strong spatio-temporal gradients. Abrupt changes in species concentrations arise where distinct airmasses meet, whether as vertical layers or horizontal fronts. The factors that generate and shift the airmass boundaries implied by the hourly data have yet to be determined.

- Some of the worst haze near the Grand Canyon is associated with transport from Southern California and the regions to the south of Grand Canyon. The results of these analyses do not support a more quantitative apportionment of source contributions, although the modified CMB analyses (see Section 8.5.3) do address this issue. Hourly tags are unavailable for some potentially significant haze sources, such as nearby Las Vegas, California's San Joaquin Valley, and northern Mexico. Moreover, some of the observed association with distant emissions could reflect enhanced conversion of local emissions in a more reactive background.

The MPP emissions impact at a receptor will be as both primary and secondary particles. With very few assumptions, the MPP tracer data can be used to make reliable estimates of the MPP contribution of primary fine particulate matter at any of the tracer monitoring sites. This is accomplished by multiplying the measured ambient MPP tracer concentrations by the ratio of primary particulate to tracer emission rates for MPP. Assumptions include (1) a constant fine particulate matter to tracer ratio, which is approximately correct except when the electrostatic

precipitators are not functioning normally, and (2) no depositional loss of the fine particulate matter during transport from MPP to the monitoring sites, which is reasonable except under precipitation conditions. The ratio of tracer to fine particulate matter emission rates is determined from in-stack measurements of fine particulate matter and $SO_x$ concentrations (Eatough, 1993) combined with the ratio of tracer to $SO_x$ emission rates that was kept nearly constant as part of the study design. Using this method, the maximum 12-hour duration primary particulate mass concentration contributed by MPP at Meadview is about 190 ng/$m^3$. This corresponds to a maximum fraction of measured fine mass concentration of about 4% and a maximum fraction of measured light extinction of about 1.8%, where the light extinction is calculated using 3 $m^2$/g as the extinction efficiency. Corresponding maximum 12-hour duration values at Hopi Point are much smaller.

An alternative means of estimating the primary particle impact is from measurements of spherical aluminosilicate (SAS) particle concentration measurements at Meadview. Assuming that all SAS particles measured at Meadview originated from MPP (which makes this estimate higher than actual), primary particle mass from MPP was less than or equal to 30 ng/$m^3$ for all 12-hour sampling periods during the summer intensive. This corresponds to an extinction impact at Meadview due to primary MPP emissions of less than 0.1 $Mm^{-1}$, or less than 0.4% of the total extinction. These values are even smaller than those estimated from the tracer scaling.

The duration of MPP plume impacts is also of interest. A limited amount of high-time resolution tracer monitoring data is available at the Meadview monitoring site for several weeks during the summer intensive period (from July 28 to Aug. 14). Data gaps nearly every day caused by short-term periodic power outages make the data record far from ideal, however it is sufficient to provide some insights into the duration and timing of MPP plume impacts at Meadview in late summer. Figure 9-4, a time plot of the $20^{th}$, $50^{th}$, and $80^{th}$ percentile of hourly tracer data shows that the MPP tracer tends to be greatest at Meadview in the mid-afternoon and evening hours during the summer intensive. That is not to say that the MPP plume exclusively reached Meadview during these hours. For example the $80^{th}$ percentile points indicate that peaks can occur in the early and mid-morning hours.

Appendix B contains a brief description of the method used to estimate the duration of the MPP emissions impacts at Meadview during the summer. Determining the typical duration of the presence of MPP emissions at Meadview is complicated by the inability of the high-time resolution tracer monitor to reliably differentiate background tracer levels from those just above background and by the data gaps on many of the days. The range of impact duration estimates is from about 4 hours to 16 hours depending primarily on the day and to a lesser extent on the assumptions used in the estimation method. For the 14 days with sufficient high-time resolution tracer data, a mean and standard deviation of 8.2 $\pm$ 3.4 hours results from using the assumption that the impact duration is estimated to be twice the minimum time required to accumulate half of the day's cumulative dose.

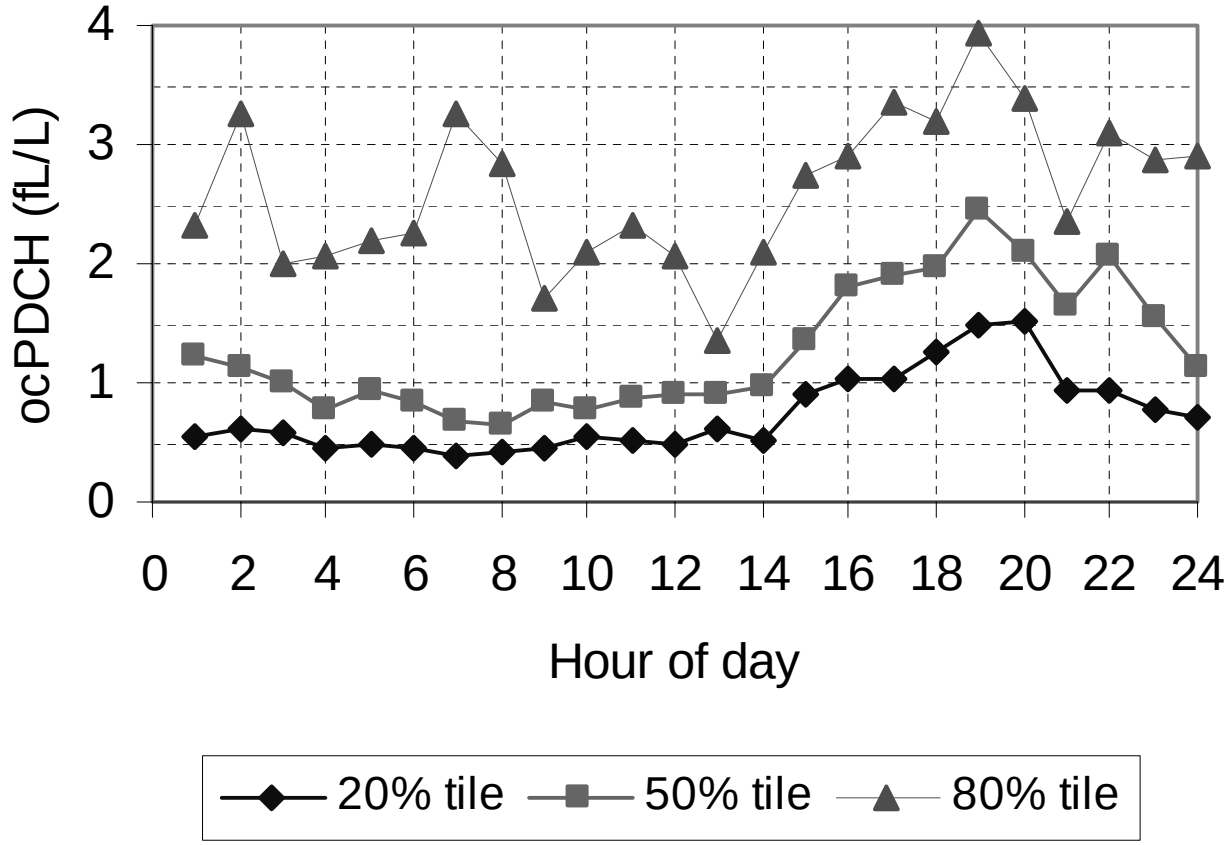


*Figure 9-4 20th, 50th, and 80th percentile ocPDCH tracer concentration at Meadview by hour of day, July 28- August 14, 1992. Concentration includes a background of about 0.5 fl/l.*

**9.4 What is a likely range of 12-hour MPP contributions to GCNP sulfate during the intensive monitoring periods?**

Methods described in Section 8.3 were used to estimate the sulfate contribution of MPP at Meadview and Hopi Point monitoring sites. As indicated in Section 8.4 (and also in Table 9-2 later in this section) the results of the various methods do not agree well on a sample period by sample period basis. Though it would be useful to identify one or more methods as providing the best estimates for some or all sample periods or conversely to identify methods that are thought to make poor estimates, no approach for making such determinations was agreed upon and no effort was made to rank the credibility of the methods. Therefore we present here the findings of all methods.

Because decisions on managing MPP emissions will likely turn on the frequency distribution of MPP's sulfur contributions rather than its contributions to any specific sampling period, the attribution results are presented as cumulative frequency distributions. A discussion of issues concerning this form of presentation appeared in Section 8.5. Most important, it needs to be recognized that the cumulative frequency distributions hide the fact that there are discrepancies in the sample period predictions between the various methods. Therefore, the cumulative frequency distribution presentations below should be viewed as interpretations of the modeled attribution results that were presented in Section 8.5, and should be considered less rigorous

presentations of the relative MPP contribution than the direct presentations of impacts given there.

Figure 9-5 through Figure 9-7 contain cumulative frequency distributions (CFDs) of the 12-hour estimated MPP contributions to particulate sulfate concentration by the various methods for the summer and winter intensive monitoring periods at Meadview and the summer intensive period at Hopi Point. No impact was estimated for the winter at Hopi Point.

The information on these plots portrays the basic findings of the attribution methods and of several efforts to estimate upper and lower bounds. Predictions of MPP contributions to ambient sulfate by various models are indicated with solid black points. Potential upper and lower bounds, which are not intended to represent estimates of actual MPP contributions, were determined by several methods and are indicated by open points. The methods used for attribution and for the bounding estimates are all described in section 8.3. Figure 9-5 also shows the cumulative frequency distribution of sulfate measurements at Meadview.

As might be expected, the lower-bound method that assumes only dry $SO_2$ to particulate sulfate conversion (CALPUFF Dry) generally estimates lower MPP contributions than those models that attempt to incorporate wet conversion (MCMB, DMBR, and ROME). HAZEPUFF, which has a simple algorithm for aqueous conversion sometimes predicts less sulfate than CALPUFF Dry. At the upper end of the range, the upper bound method that mandates daily wet conversion (CALPUFF Wet) produces estimates greater than those of all four of the models. Tracer Max results are shown as an ultimate upper bound but should not be considered estimates of actual conditions because the assumption of 100% of $SO_2$ to particulate sulfate conversion is extremely unlikely to be realized. However, the Tracer Max curve is useful to show how much lower the other estimates are compared to this firm upper bound result.

Not surprisingly, results of the various modeling methods tend to agree more closely for the lower percentile MPP impact estimates, which are ultimately bounded by zero impact, and they depart most in their estimates at the upper extreme of impact. One cause for this expansion of the range among methods at higher estimated MPP impact values is the variation between the methods' approaches to estimate the fraction of $SO_2$ converted to particulate sulfate. While some methods have very simplistic approaches to estimate conversion and others are more complex, there is no simple way to determine which yield the better result. Just as the range among results expands at the higher impact extreme, it is reasonable to expect that the uncertainty limits increase for any of the estimates as the predictions approach the upper level extreme values for that method. With this in mind, most of the material presented below will focus on the range of MPP estimated impacts for the $50^{th}$ and $90^{th}$ percentiles cumulative frequencies.

Shown in Table 9-1 are the ranges of $50^{th}$ and $90^{th}$ percentile values of particulate sulfate estimated by the various methods. Bounding estimates, excluding Tracer Max, are also given in parentheses. Estimated sulfate contributions by MPP are greatest at Meadview in both seasons and greatest in the summer at both sites. As pointed out above, the high end of the range for Meadview for summer is established by CALPUFF Wet bounding results. This method's assumption of wet conversion for each 12-hour estimate is less likely to be correct for conditions below about the mid-point of the cumulative frequency distribution ($50^{th}$ percentile) than above it

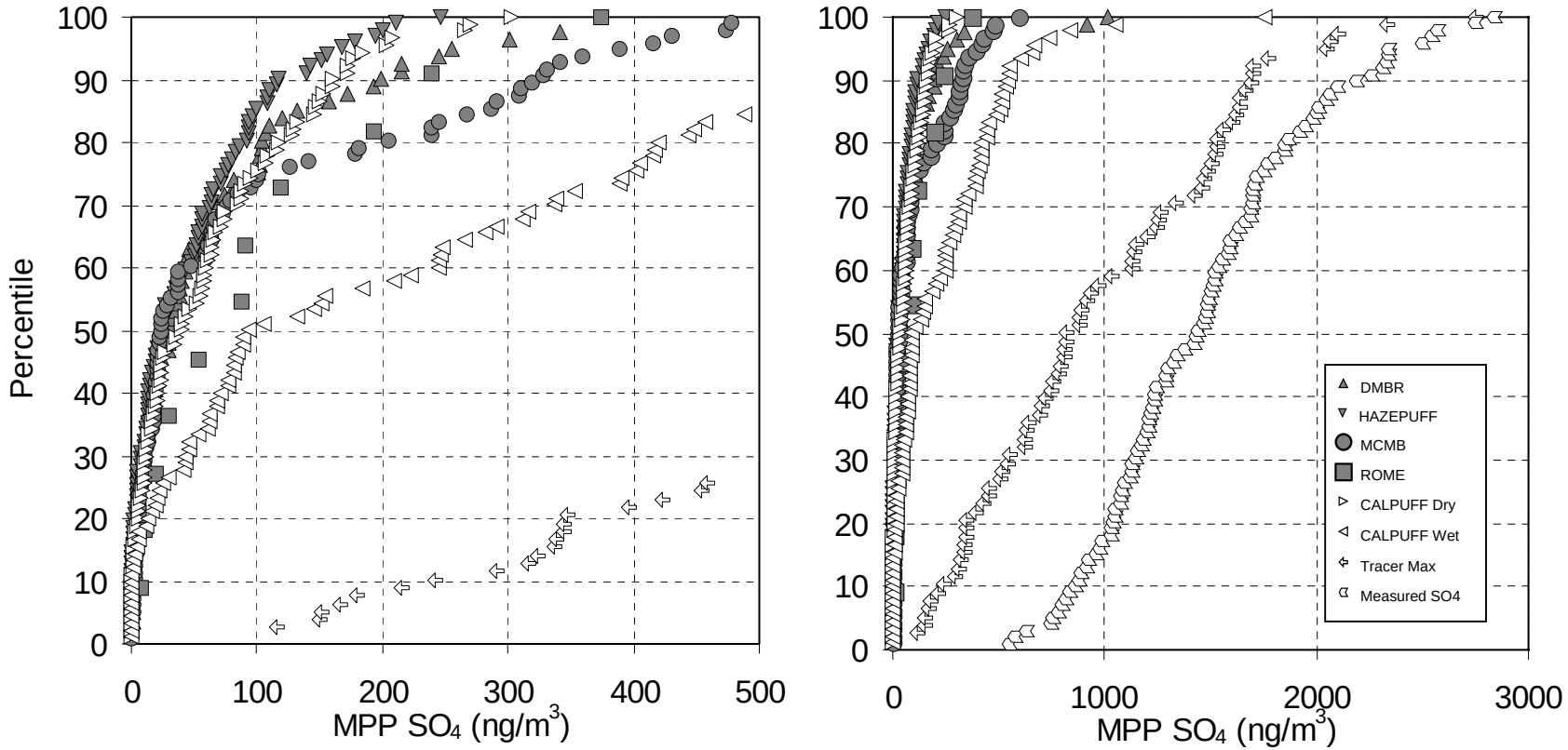


*Figure 9-5 Cumulative frequency plots of 12 hour sulfate attribution to MPP at Meadview during the summer intensive. Filled symbols represent estimates of MPP attribution; open symbols indicate bounding calculations and physical upper bounds. Note: Inconsistent modeling results can yield similar frequency distributions.*

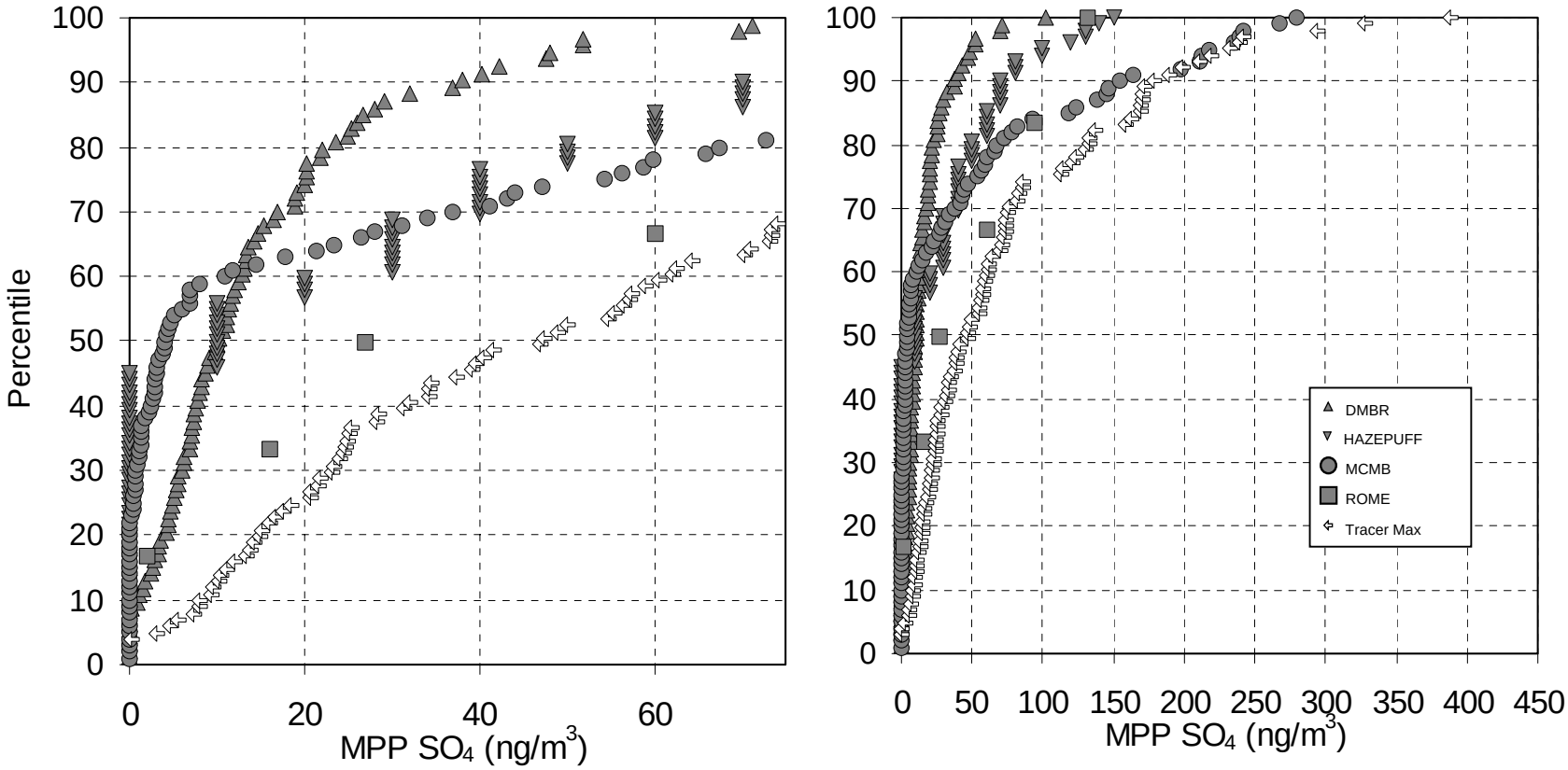


*Figure 9-6 Cumulative frequency plots of 12 hour sulfate attribution to MPP at Hopi Point during the summer intensive. Filled symbols represent estimates of MPP attribution; open symbols indicate bounding calculations. Note: Inconsistent modeling results can yield similar frequency distributions.*

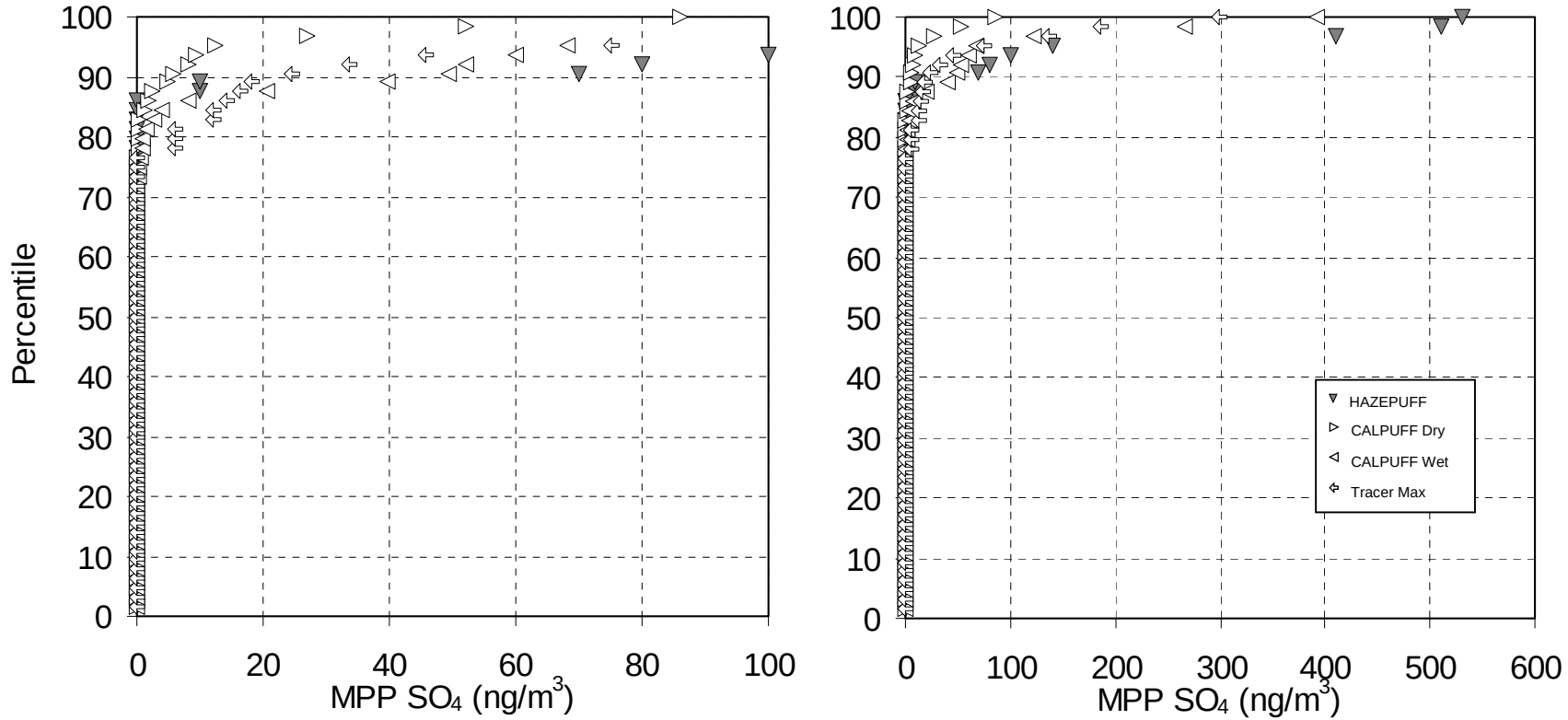


*Figure 9-7 Cumulative frequency plots of 12 hour sulfate attribution to MPP at Meadview during the winter intensive. Filled symbols represent estimates of MPP attribution; open symbols indicate bounding calculations. Note: Inconsistent modeling results can yield similar frequency distributions.*

because clouds were few or not present as often as half of the time (Ames et al., 1998). Surprisingly, the high end of the 90th percentile range for Meadview during the winter intensive was established by the MCMB method, which slightly exceeded the CALPUFF Wet bounding estimates. If the MCMB results are credible then the $SO_2$ to particulate sulfate conversion during the winter must occasionally exceed that assumed by CALPUFF Wet.

*Table 9-1 Range of estimated 12-hour MPP sulfate (ng/m$^3$) for the 50th and 90th percentile conditions. Model attribution results excluding the bounding estimates of CALPUFF Wet and Dry are shown in bold. Values in parentheses represent the ranges of all attribution results.*

| | Winter | | Summer | |
|---|---|---|---|---|
| | 50th | 90th | 50th | 90th |
| Meadview | (0.0 to 0.0) | 40 (5 to 50) | **23** to **71 (**23 to 93) | **120** to **320** (120 to 540) |
| Hopi Point | (0.0 to 0.0) | (0.0 to 0.0) | **4** to **27** | **38** to **160** |

In order to estimate the relative importance of MPP compared to all other sources of particulate sulfate, each estimate of MPP-contributed particulate sulfate was divided by the measured sulfate concentration for the corresponding sample period. Cumulative frequency distribution plots of the estimated relative contribution of particulate sulfate by MPP are shown in Figure 9-8 through Figure 9-10. These curves look similar to those in the Figure 9-5 through Figure 9-7, with the ordering from highest to lowest estimates of the various methods being the same over most of the percentile values. It should be recognized, however, that the various points on a single frequency distribution curve may have been reordered, since a given concentration can represent a small fraction of a large measured value or a large fraction of a small measured value.

The qualitative similarity of the curves for absolute and relative concentrations suggests that there are no systematic relationships between the MPP impact estimates by the various methods and the ambient sulfate concentrations which are the denominators of the relative concentrations. This is confirmed by the correlation coefficients between predictions by the various methods and measured particulate sulfate at Meadview during the summer shown in Table 9-2.

One point exceeds 100% in Figure 9-8, a CALPUFF Wet bounding estimate of about 1700 ng/m$^3$ on a day with measured sulfate of about 1600 ng/m$^3$. All other estimates are well below Tracer Max.

As expected from the previous discussion of meteorology, Meadview in either season has larger estimated fractional MPP contributions at the 50th and 90th percentile than at Hopi Point, and the summer intensive period ranges exceed those of the winter intensive for both sites (see

Table 9-3). Notice that the high end of the 50th percentile range for the estimated MPP fraction of particulate sulfate at Meadview during the summer intensive monitoring period is roughly half of the upper limit of possible average MPP impact determined in the "outage study" (8% compared to 15%) reported by Murray et al. (1990) and discussed in Section 9.2.

*Table 9-2 Cross-correlation coefficients (r) for predicted MPP sulfate by the various methods and the tracer concentrations, measured sulfate and transmissometer extinction coefficients for summer at Meadview. Numbers of data pairs are shown in the second table below.*

| | MCMB | HAZE PUFF | DMBR | CALPUFF Dry | CALPUFF Wet | TMBR | TAGIT | ROME | SO4 | Tracer Max | ocPDCH | $b_{ext}$ |
|---|---|---|---|---|---|---|---|---|---|---|---|---|
| MCMB | 1.00 | | | | | | | | | | | |
| HAZEPUFF | 0.03 | 1.00 | | | | | | | | | | |
| DMBR | 0.24 | 0.22 | 1.00 | | | | | | | | | |
| CALPUFF Dry | 0.43 | 0.14 | 0.28 | 1.00 | | | | | | | | |
| CALPUFF Wet | 0.29 | 0.15 | 0.60 | 0.75 | 1.00 | | | | | | | |
| TMBR | 0.45 | 0.00 | 0.70 | 0.40 | 0.56 | 1.00 | | | | | | |
| TAGIT | 0.18 | 0.11 | 0.07 | -0.04 | -0.13 | 0.06 | 1.00 | | | | | |
| ROME | 0.46 | -0.18 | -0.08 | 0.16 | -0.08 | 0.02 | -0.04 | 1.00 | | | | |
| SO4 | 0.14 | 0.00 | 0.16 | -0.01 | 0.02 | 0.24 | 0.56 | 0.25 | 1.00 | | | |
| tracer max | 0.37 | 0.03 | 0.42 | 0.38 | 0.37 | 0.71 | 0.16 | 0.58 | 0.56 | 1.00 | | |
| ocPDCH | 0.45 | -0.01 | 0.69 | 0.39 | 0.56 | 1.00 | 0.02 | 0.04 | 0.23 | 0.71 | 1.00 | |
| $b_{ext}$ | -0.18 | -0.27 | -0.04 | -0.38 | -0.24 | -0.11 | 0.44 | -0.18 | 0.67 | 0.06 | -0.12 | 1.00 |

| | MCMB | HAZE PUFF | DMBR | CALPUFF Dry | CALPUFF Wet | TMBR | TAGIT | ROME | SO4 | Tracer Max | OcPDCH | $b_{ext}$ |
|---|---|---|---|---|---|---|---|---|---|---|---|---|
| MCMB | 96 | | | | | | | | | | | |
| HAZEPUFF | 96 | 102 | | | | | | | | | | |
| DMBR | 79 | 81 | 81 | | | | | | | | | |
| CALPUFF Dry | 87 | 90 | 81 | 90 | | | | | | | | |
| CALPUFF Wet | 87 | 90 | 81 | 90 | 90 | | | | | | | |
| TMBR | 79 | 81 | 81 | 81 | 81 | 81 | | | | | | |
| TAGIT | 36 | 39 | 31 | 34 | 34 | 30 | 39 | | | | | |
| ROME | 11 | 11 | 11 | 11 | 11 | 11 | 3 | 11 | | | | |
| SO4 | 94 | 99 | 78 | 87 | 87 | 78 | 37 | 11 | 99 | | | |
| tracer max | 77 | 78 | 78 | 78 | 78 | 78 | 32 | 11 | 78 | 78 | | |
| ocPDCH | 79 | 81 | 81 | 81 | 81 | 81 | 32 | 11 | 78 | 78 | 81 | |
| $b_{ext}$ | 96 | 102 | 81 | 90 | 90 | 81 | 39 | 11 | 99 | 78 | 81 | 102 |

*Table 9-3 Range of estimated 12-hour MPP fraction of measured sulfate (%) for the 50th and 90th percentile conditions. Model attribution results excluding the bounding estimates of CALPUFF Wet and Dry are shown in bold. Values in parentheses represent the ranges of all attribution results.*

| | Winter | | Summer | |
|---|---|---|---|---|
| | 50th | 90th | 50th | 90th |
| Meadview | (0.0 to 0.0) | **3.5** (0.7 to 4.8) | **1.7** to **3.3** (1.7 to 8.0) | **8.7** to **21** (8.7 to 42) |
| Hopi Point | (0.0 to 0.0) | (0.0 to 0.0) | **0.4** to **1.6** | **3.1** to **13** |

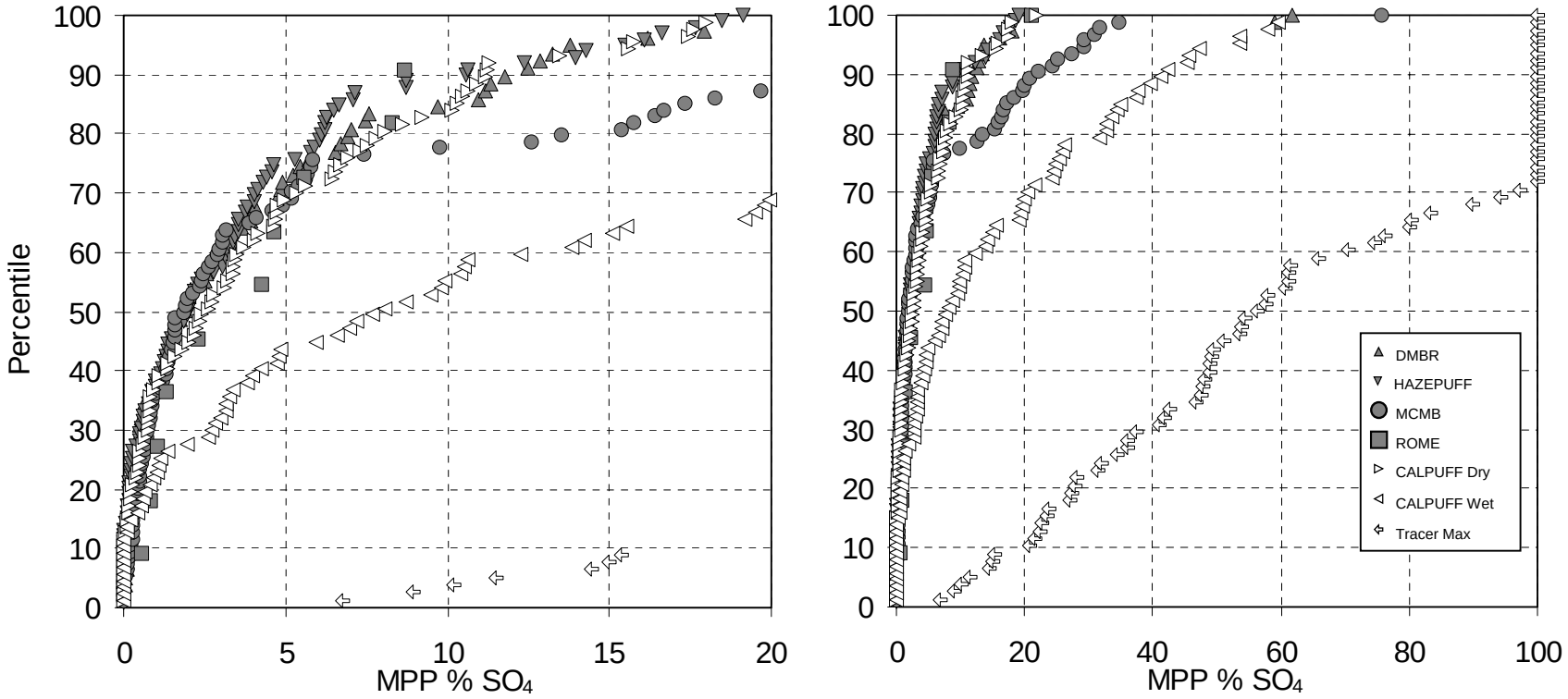


*Figure 9-8 Cumulative frequency distributions of 12-hour estimated MPP percentage contributions to particulate sulfate concentration at Meadview during the summer intensive. Filled symbols represent estimates of MPP attribution; open symbols indicate bounding calculations. Note: Inconsistent modeling results can yield similar frequency distributions.*

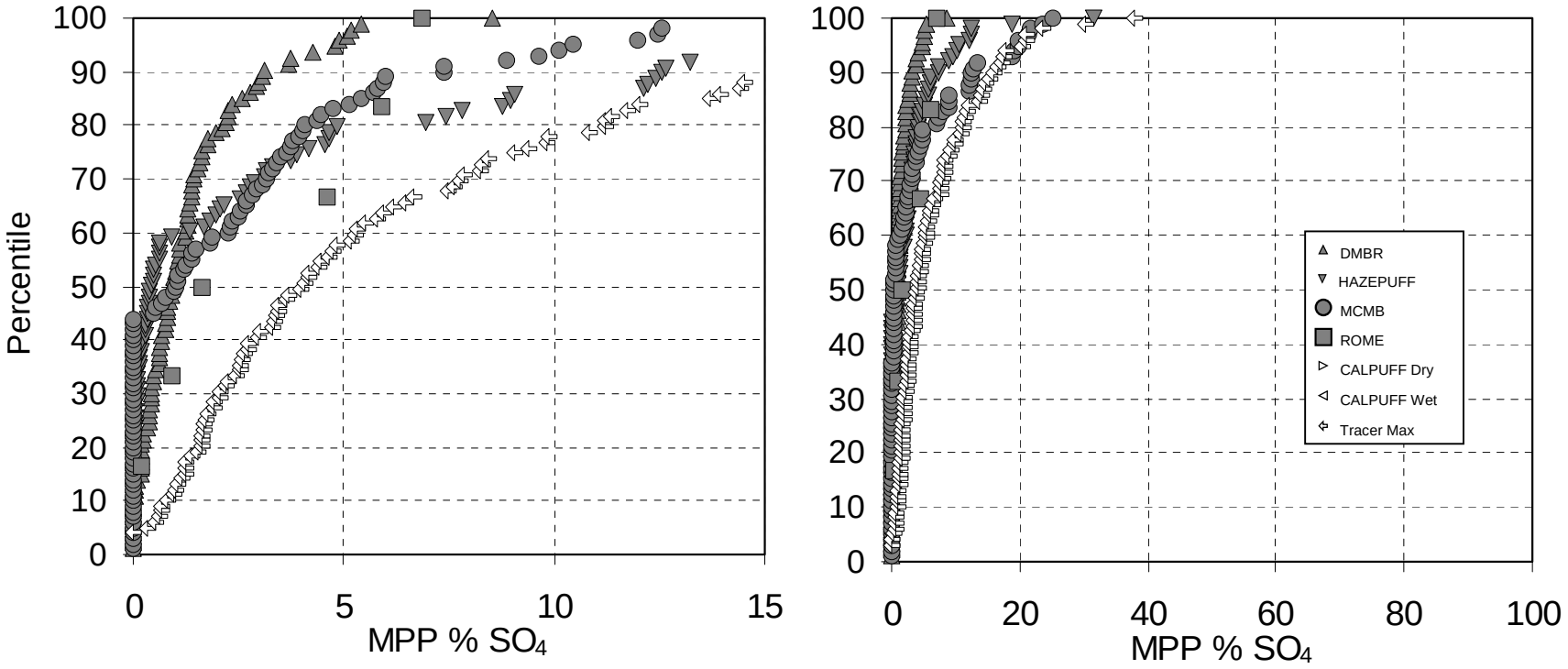


*Figure 9-9 Cumulative frequency distributions of 12-hour estimated MPP percentage contributions to particulate sulfate concentration at Hopi Point during the summer intensive. Filled symbols represent estimates of MPP attribution; open symbols indicate bounding calculations. Note: Inconsistent modeling results can yield similar frequency distributions.*

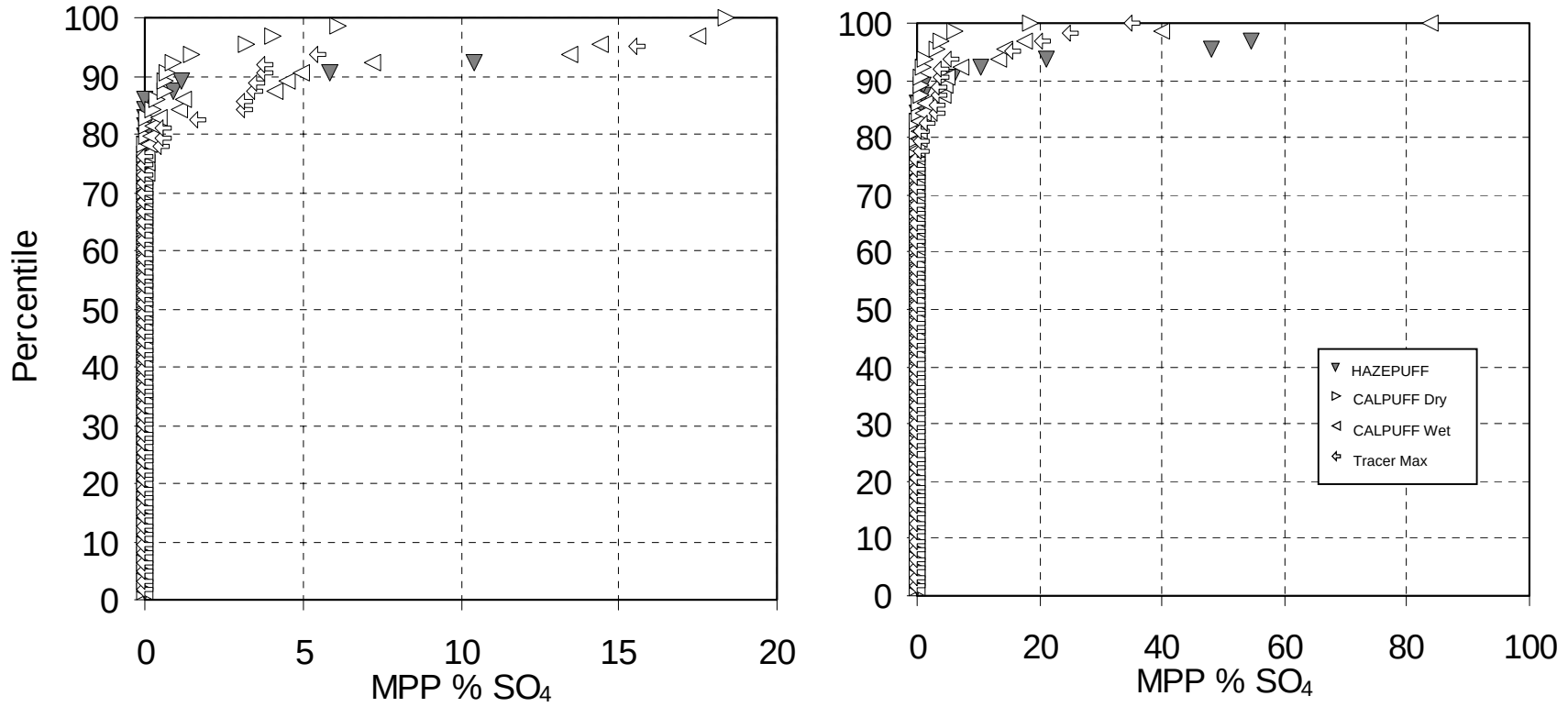


*Figure 9-10 Cumulative frequency distributions of 12-hour estimated MPP percentage contributions to particulate sulfate concentration at Meadview during the winter intensive. Filled symbols represent estimates of MPP attribution; open symbols indicate bounding calculations. Note: Inconsistent modeling results can yield similar frequency distributions.*

## 9.5 What is a likely range of 12-hour and 24-hour MPP contributions to GCNP light extinction during the intensive monitoring periods?

As described in Equation (6-6) in Section 6.2, the amount of light extinction coefficient contributed by particulate sulfate can be estimated by multiplying the ammonium sulfate concentration expressed in micrograms per cubic meter by 2 times an appropriate water growth function of relative humidity. This method was used to convert estimates of MPP-contributed particulate sulfate to estimates of MPP-contributed light extinction coefficient for both monitoring sites and intensive monitoring seasons. As was pointed out in Section 8.4.3, the perceptibility of a change in haze depends on many factors, but for many situations a fractional change in light extinction coefficient is a reasonably linear index for haziness. Accordingly, estimates of MPP-contributed haze were divided by the corresponding light extinction coefficient values to produce estimates of fractional changes in light extinction coefficient due to MPP.

Cumulative frequency distributions of the estimates of 12-hour MPP-contributed fractional light extinction coefficient are shown in Figure 9-11 through Figure 9-13, where transmissometer measurements were the source of the total light extinction coefficient. The shapes and relative positions of the various curves are not much changed from the corresponding particulate sulfate cumulative distribution curves. Again this is probably due to a lack of a strong correlation between the 12-hour estimated MPP contributions and the measured extinction coefficient, as reflected in Table 9-1.

The ranges of estimated MPP fractional contribution at the 50$^{th}$ and 90$^{th}$ percentile frequencies corresponding to the methods shown in Figure 9-11 through Figure 9-13 are summarized in Table 9-4. To gain appreciation for the perceptibility of changes corresponding to the fractional change in light extinction coefficient shown in the table, view the set of computer generated photos in the back of the report and described in Section 9.8.

*Table 9-4 Range of estimated 12-hour MPP fraction (%) of measured light extinction coefficient for the 50th and 90th percentile conditions. Model attribution results excluding the bounding estimates of CALPUFF Wet and Dry are shown in bold. Values in parentheses represent the ranges of all attribution results.*

| | Winter | | Summer | |
|---|---|---|---|---|
| | 50$^{th}$ | 90th | 50$^{th}$ | 90$^{th}$ |
| Meadview | (0.0 to 0.0) | **0.1** (0.1 to 0.4) | **0.2** to **0.6** (0.2 to 1.0) | **1.3** to **2.8** (1.3 to 5.0) |
| Hopi Point | (0.0 to 0.0) | (0.0 to 0.0) | **0.1** to **0.4** | **0.5** to **2.6** |

As was mentioned in Section 5.4.4 and Section 6.2, there is a concern that the Meadview transmissometer-measured light extinction coefficient may be systematically too large. To explore how much this would affect the results shown in Figure 9-11 through Figure 9-13 and summarized in Table 9-4, the MPP fractional contributions to light extinction coefficient values for each method were recalculated using calculated extinction instead of the transmissometer measurements. The calculated extinction should generally slightly underestimate the true light extinction coefficient (See Section 5.4.4). The results of this are displayed in Figure 9-14 through Figure 9-16 and summarized in Table 9-5. The most substantial change resulting from the use of calculated in place of transmissometer-measured light extinction coefficient is at

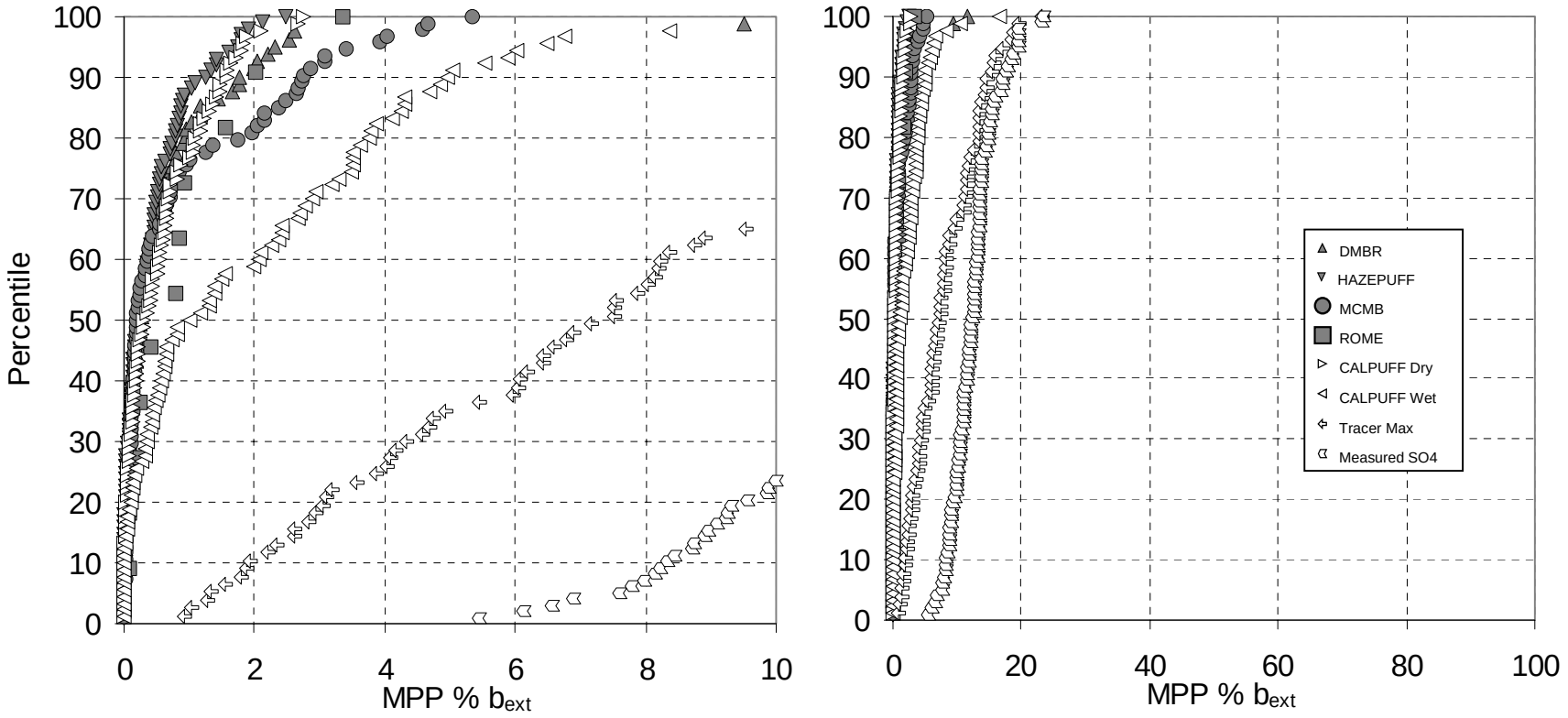


*Figure 9-11 Cumulative frequency distributions of 12-hour estimated MPP percentage contributions to measured light extinction at Meadview during the summer intensive. Filled symbols represent estimates of MPP attribution; open symbols indicate bounding calculations and physical upper bounds. Note: Inconsistent modeling results can yield similar frequency distributions.*

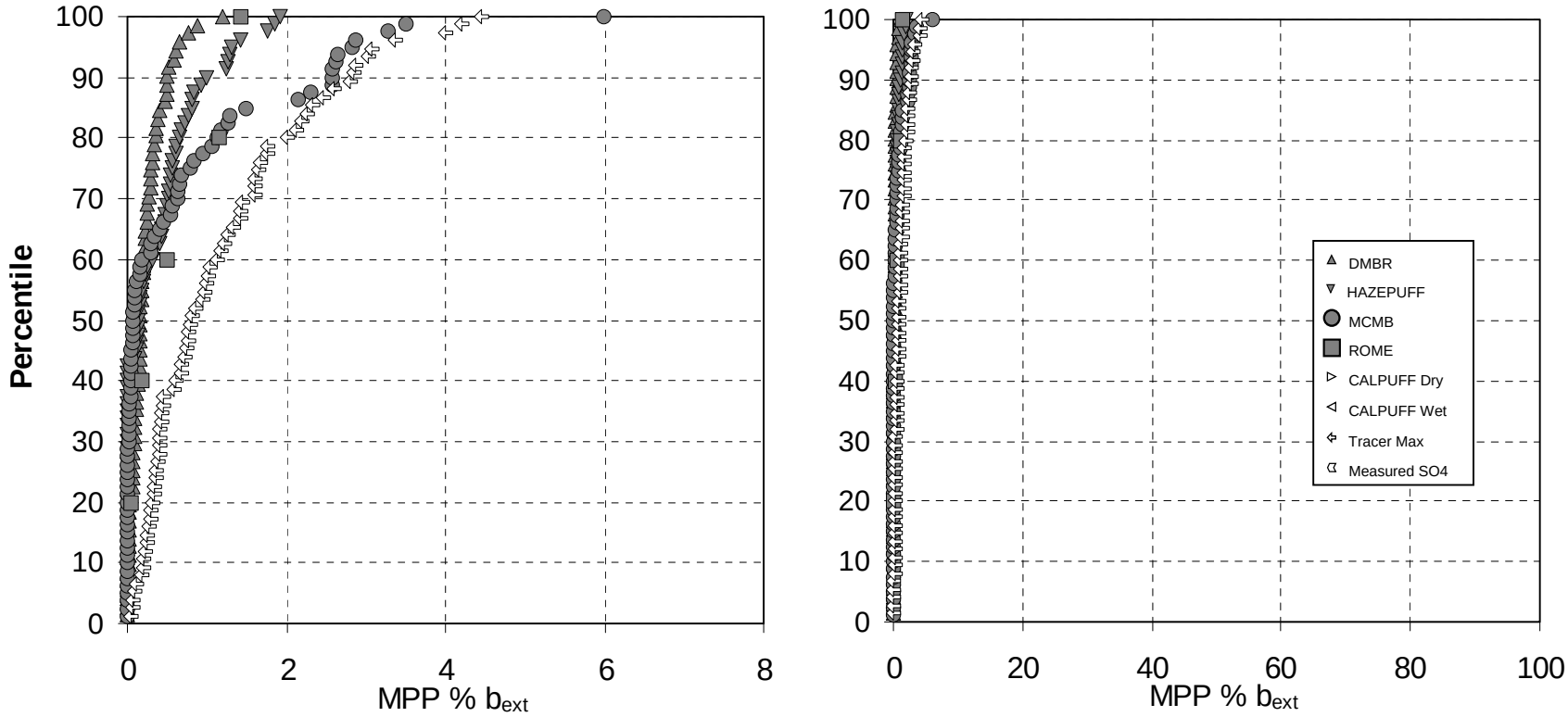


*Figure 9-12 Cumulative frequency distributions of 12-hour estimated MPP percentage contributions to measured light extinction at Hopi Point during the summer intensive. Filled symbols represent estimates of MPP attribution; open symbols indicate bounding calculations. Note: Inconsistent modeling results can yield similar frequency distributions.*

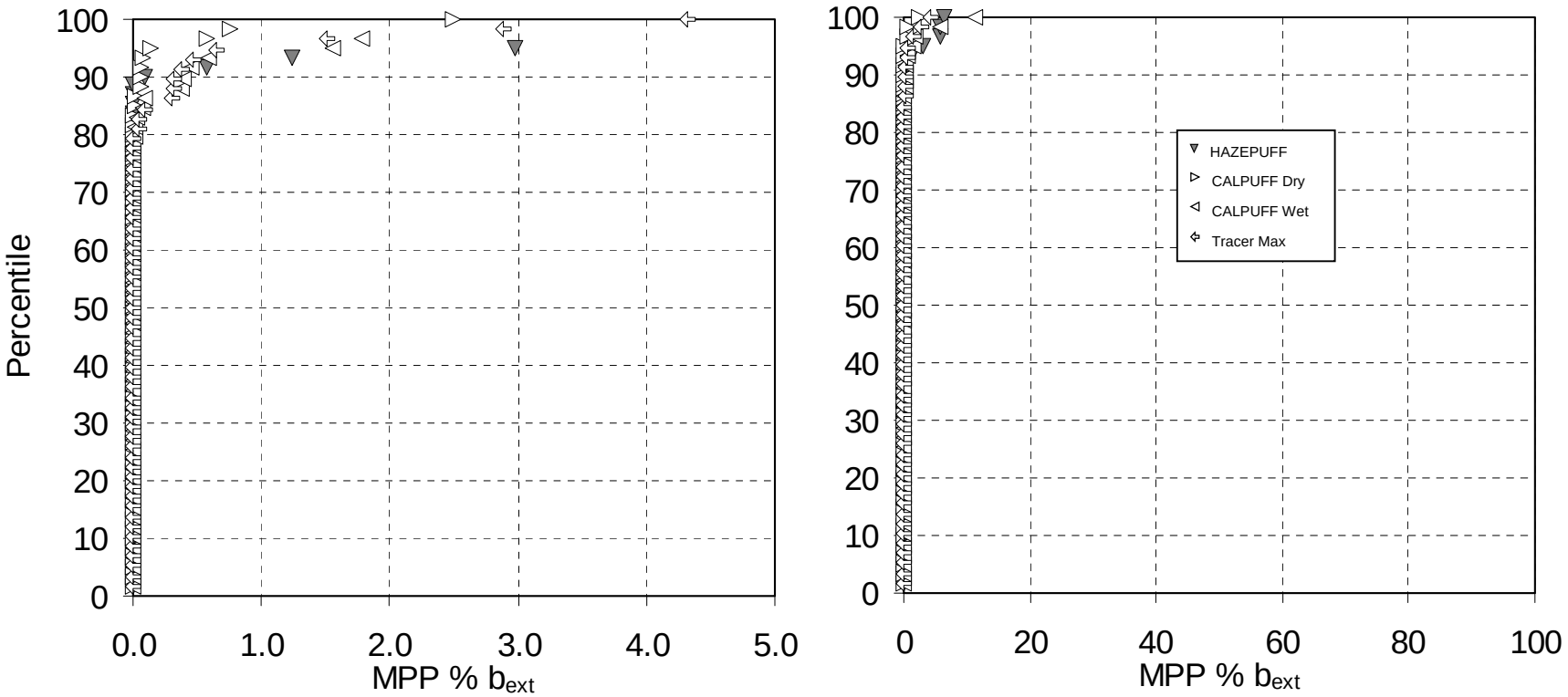


*Figure 9-13 Cumulative frequency distributions of 12-hour estimated MPP percentage contributions to measured light extinction at Meadview during the winter intensive. Filled symbols represent estimates of MPP attribution; open symbols indicate bounding calculations. Note: Inconsistent modeling results can yield similar frequency distributions.*

Meadview during the summer where the range is larger by about one third to one half using the calculated values.

*Table 9-5 Range of estimated 12-hour MPP fraction (%) of calculated light extinction coefficient for the 50th and 90th percentile conditions. Model attribution results excluding the bounding estimates of CALPUFF Wet and Dry are shown in bold. Values in parentheses represent the ranges of all attribution results.*

| | Winter | | Summer | |
|---|---|---|---|---|
| | 50th | 90th | 50th | 90th |
| Meadview | (0.0 to 0.0) | **0.2** (0.1 to 0.4) | **0.3** to **0.8** (0.3 to 1.2) | **1.9** to **4.0** (1.9 to 6.7) |
| Hopi Point | (0.0 to 0.0) | (0.0 to 0.0) | **0.1** to **0.3** | **0.6** to **2.3** |

TAGIT results have not been shown in the figures and tables thus far, because TAGIT is only able to provide 24-hour estimates while all other methods can provide 12-hour estimates. The 12-hour results for all methods can be combined to produce 24-hour results so that they can be compared with those from TAGIT. Cumulative frequency distribution curves of the estimated fraction of MPP contribution to 24-hour transmissometer-measured light extinction coefficient are shown in Figure 9-17 through Figure 9-19 and summarized in Table 9-6.

*Table 9-6 Range of estimated 24-hour MPP fraction (%) of measured light extinction coefficient for the 50th and 90th percentile conditions. Model attribution results excluding the bounding estimates of CALPUFF Wet and Dry are shown in bold. Values in parentheses represent the ranges of all attribution results..*

| | Winter | | Summer | |
|---|---|---|---|---|
| | 50th | 90th | 50th | 90th |
| Meadview | (0.0 to 0.0) | **0.0** to **0.4** | **0.3** to **0.6** (0.3 to 1.5) | **0.9** to **3.5** (0.9 to 4.8) |
| Hopi Point | (0.0 to 0.0) | (0.0 to 0.0) | **0.0** to **0.4** | **1.1** to **5.3**[1] |

Comparing corresponding curves in Figure 9-11 through Figure 9-13 and Figure 9-17 through Figure 9-19 shows that, at the high end of the distribution, the 12-hour estimated values will generally be greater than their counterpart 24-hour estimated values because the highest 12-hour values are not necessarily in the same 24-hour period. Except for reducing the highest values somewhat the corresponding curves in the two figures are very similar.

The addition of TAGIT provides a feature not seen in the results of the other methods, negative estimates of contribution by MPP. These values indicate that nearby monitoring sites with little or no MPP tracer had somewhat higher particulate sulfate on average than at the receptor site for some days. They should be interpreted as near-zero contribution by MPP. For Hopi Point summer, the uncertainty of TAGIT results is sufficiently large over the entire range that the results should all be considered below detection limits. TAGIT estimates for Meadview are not thought to be below detection limits of the method, however. The reader is referred to the description of TAGIT in Section 8.3.3 for a more complete explanation of the method.

As previously mentioned, extreme value estimates by any of the methods are believed to have the greatest uncertainty and should not be trusted as a true reflection of greatest MPP impacts.

[1] The TAGIT method that produced this result has substantial uncertainty as applied to MPP impacts at Hopi Point. The value associated with the next highest method for the 90th percentile is 2.5%, which seems to be a more reasonable upper limit.

However, some idea of the potential for extreme impacts can be obtained by examining the range of the greatest individual-day MPP attributions generated over the entire tracer period. The predictions of study-maximum ($100^{th}$ percentile) MPP contribution to Meadview light extinction during an individual 12-hour monitoring period was from about 2.5% to 11%, as seen in Figure 9-11. (The CALPUFF Wet bounding estimate takes this range up to 16%.) This wide range of estimates underscores the fact that the disagreement among estimates was greatest when estimating the highest 12-hour MPP contribution. Notice that even the upper end of this range is less than the Tracer Max upper bound result for the highest 12-hour estimate of about 23%. As explained in Section 8.3.1, Tracer Max yields an absolute upper bound obtained, in part, from the measured tracer concentrations. It makes the assumption that all emitted MPP sulfur is converted to sulfate without depositional loss during transport to Meadview, which eliminates any possibility of underestimation. Careful inspection of scatter plots of high time resolution optical and tracer data (e.g., Figure 9-2) was unable to detect any patterns of association that directly corroborate the higher MPP contributions at Meadview calculated by the models.

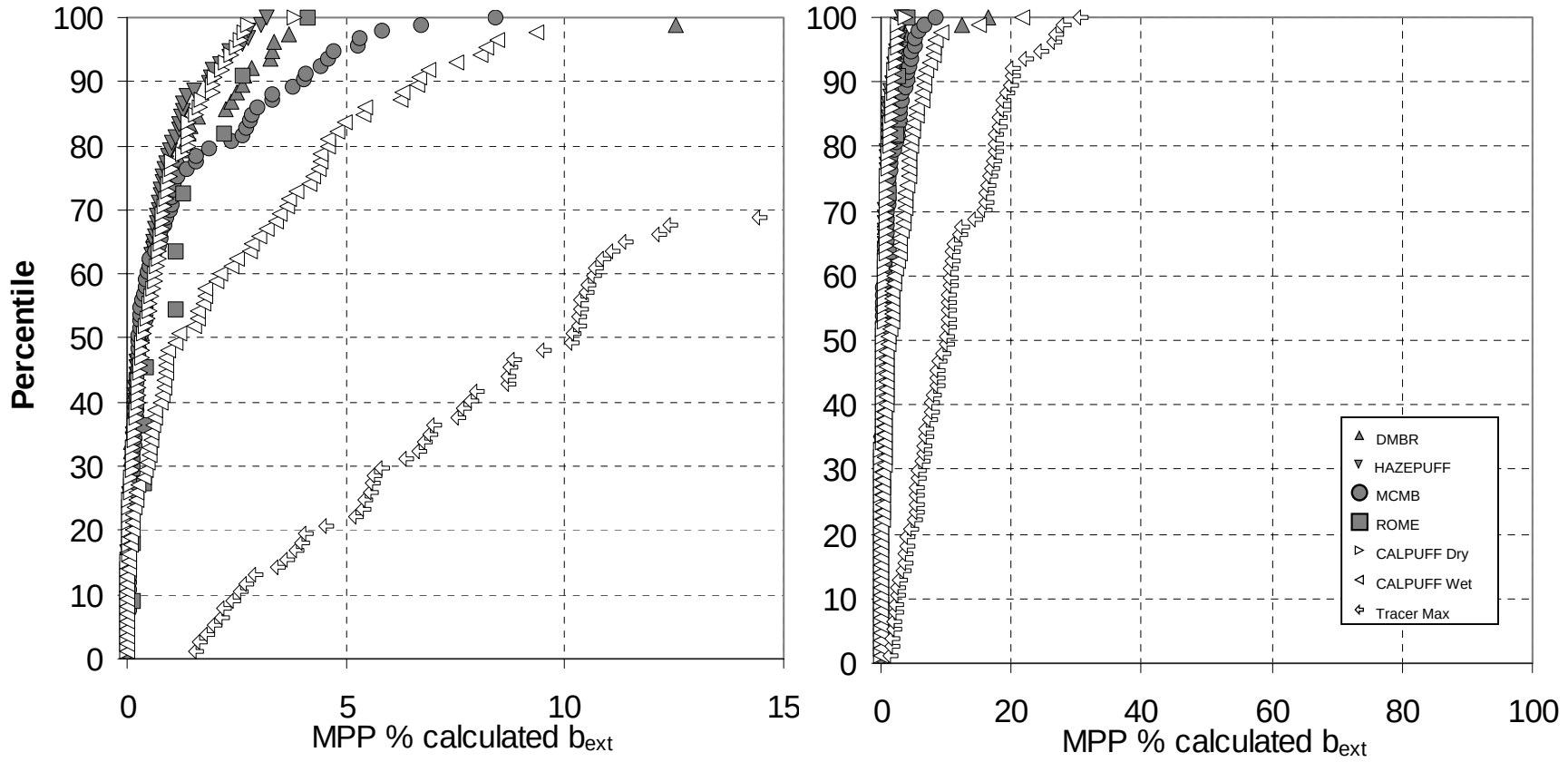


*Figure 9-14 Cumulative frequency distributions of 12-hour estimated MPP percentage contributions to calculated light extinction at Meadview during the summer intensive. Filled symbols represent estimates of MPP attribution; open symbols indicate bounding calculations. Note: Inconsistent modeling results can yield similar frequency distributions.*

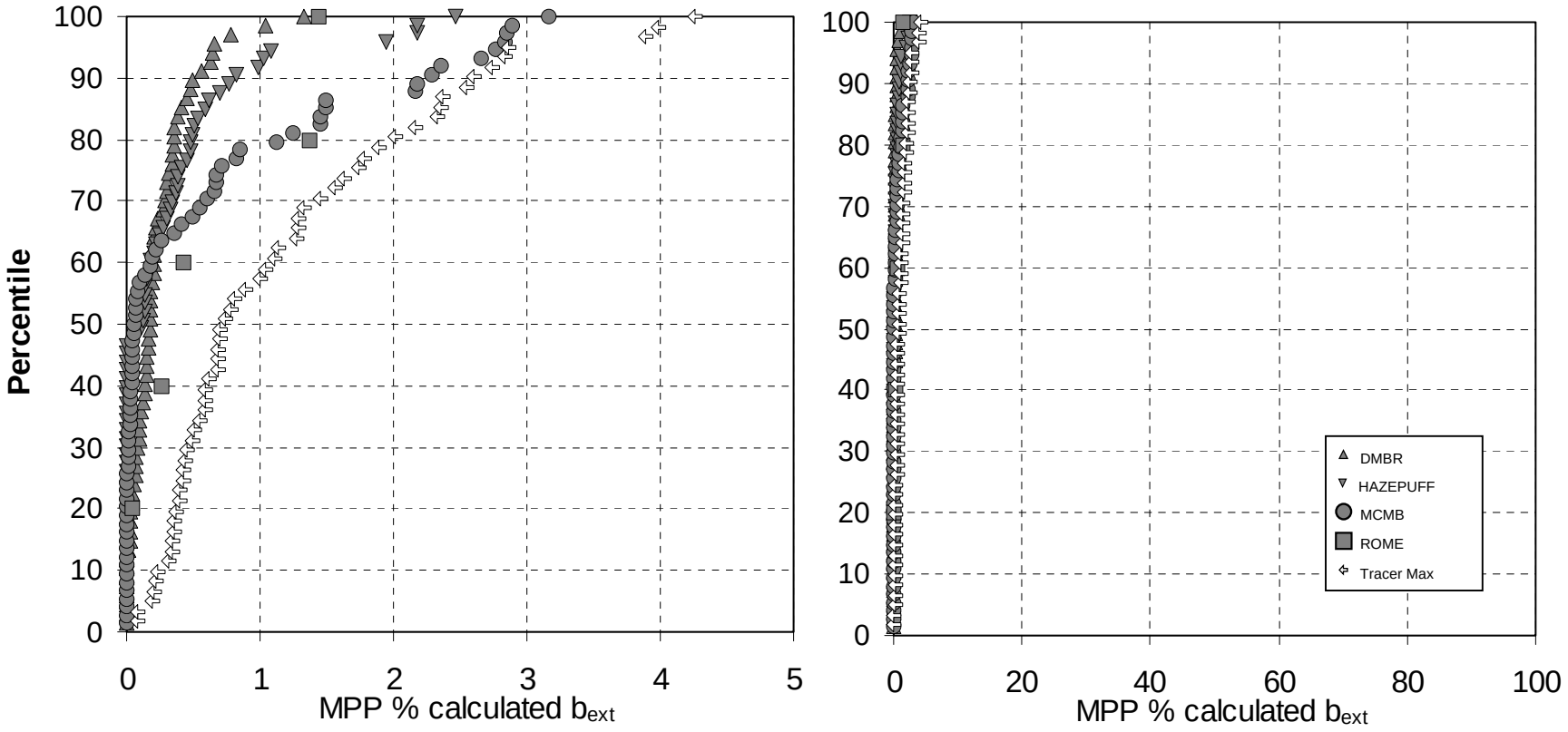


*Figure 9-15 Cumulative frequency distributions of 12-hour estimated MPP percentage contributions to calculated light extinction at Hopi Point during the summer intensive. Filled symbols represent estimates of MPP attribution; open symbols indicate bounding calculations. Note: Inconsistent modeling results can yield similar frequency distributions.*

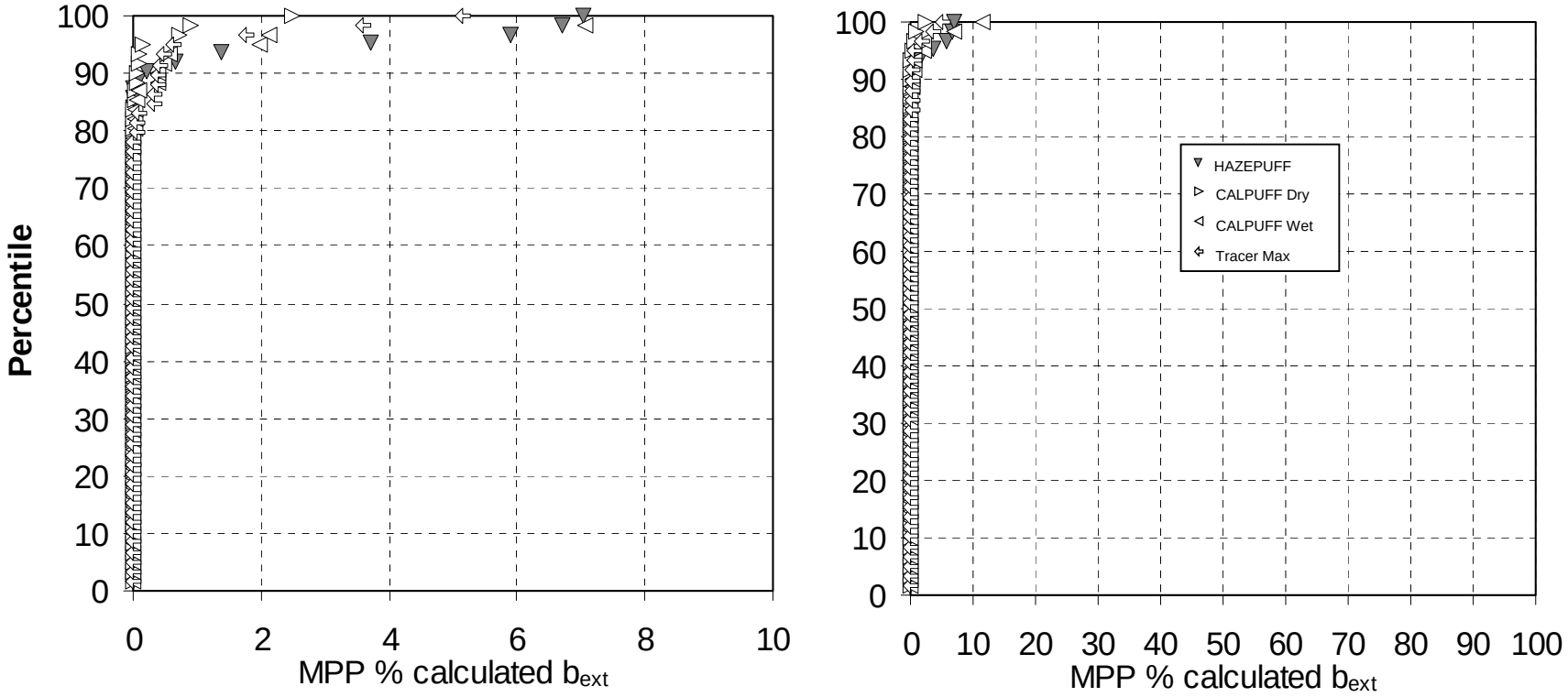


*Figure 9-16 Cumulative frequency distributions of 12-hour estimated MPP percentage contributions to calculated light extinction at Meadview during the winter intensive. Filled symbols represent estimates of MPP attribution; open symbols indicate bounding calculations. Note: Inconsistent modeling results can yield similar frequency distributions.*

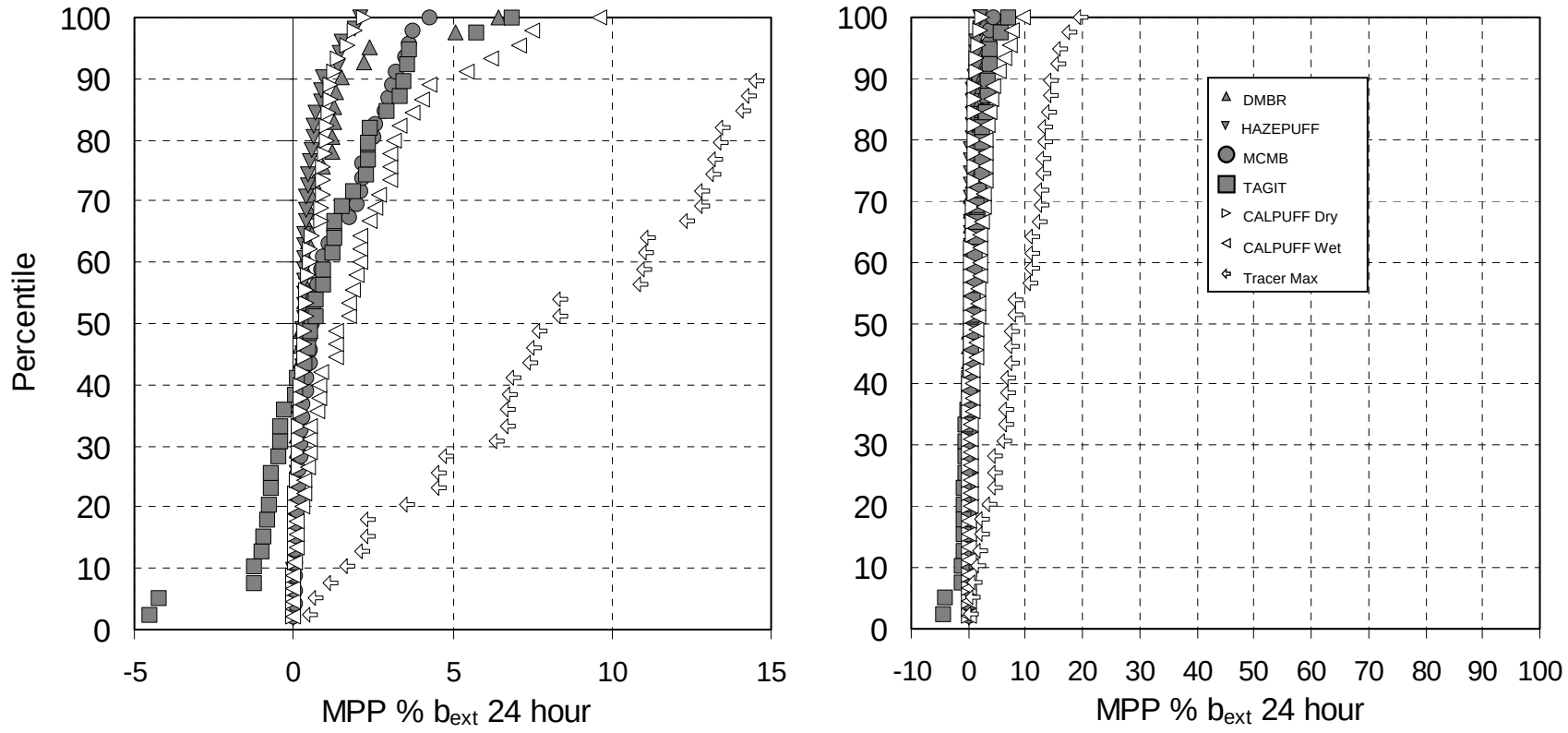


*Figure 9-17 Cumulative frequency distributions of 24-hour estimated MPP percentage contributions to measured light extinction at Meadview during the summer intensive. Filled symbols represent estimates of MPP attribution; open symbols indicate bounding calculations. Note: Inconsistent modeling results can yield similar frequency distributions.*

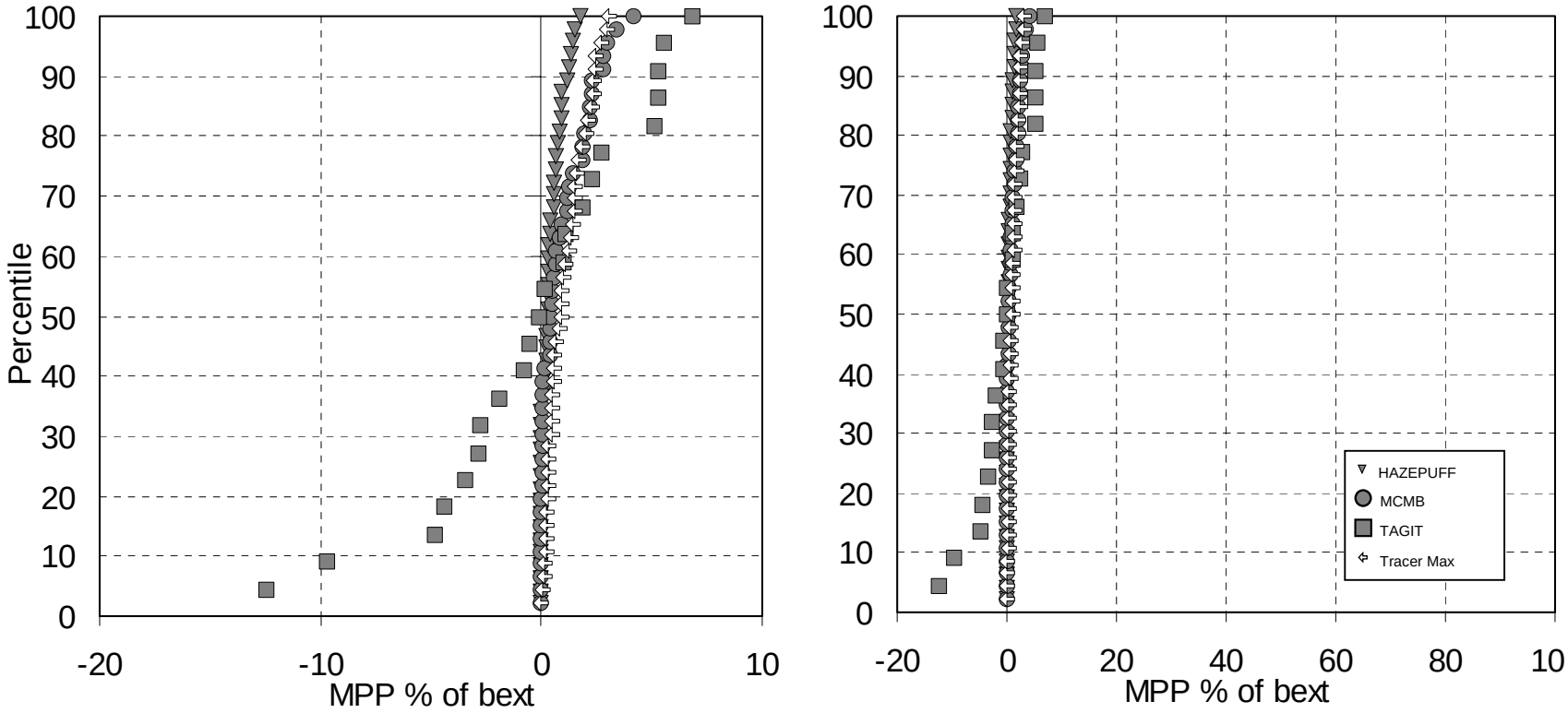


*Figure 9-18 Cumulative frequency distributions of 24-hour estimated MPP percentage contributions to measured light extinction at Hopi Point during the summer intensive. The TAGIT results for Hopi Point are highly uncertain. Filled symbols represent estimates of MPP attribution; open symbols indicate bounding calculations. Note: Inconsistent modeling results can yield similar frequency distributions.*

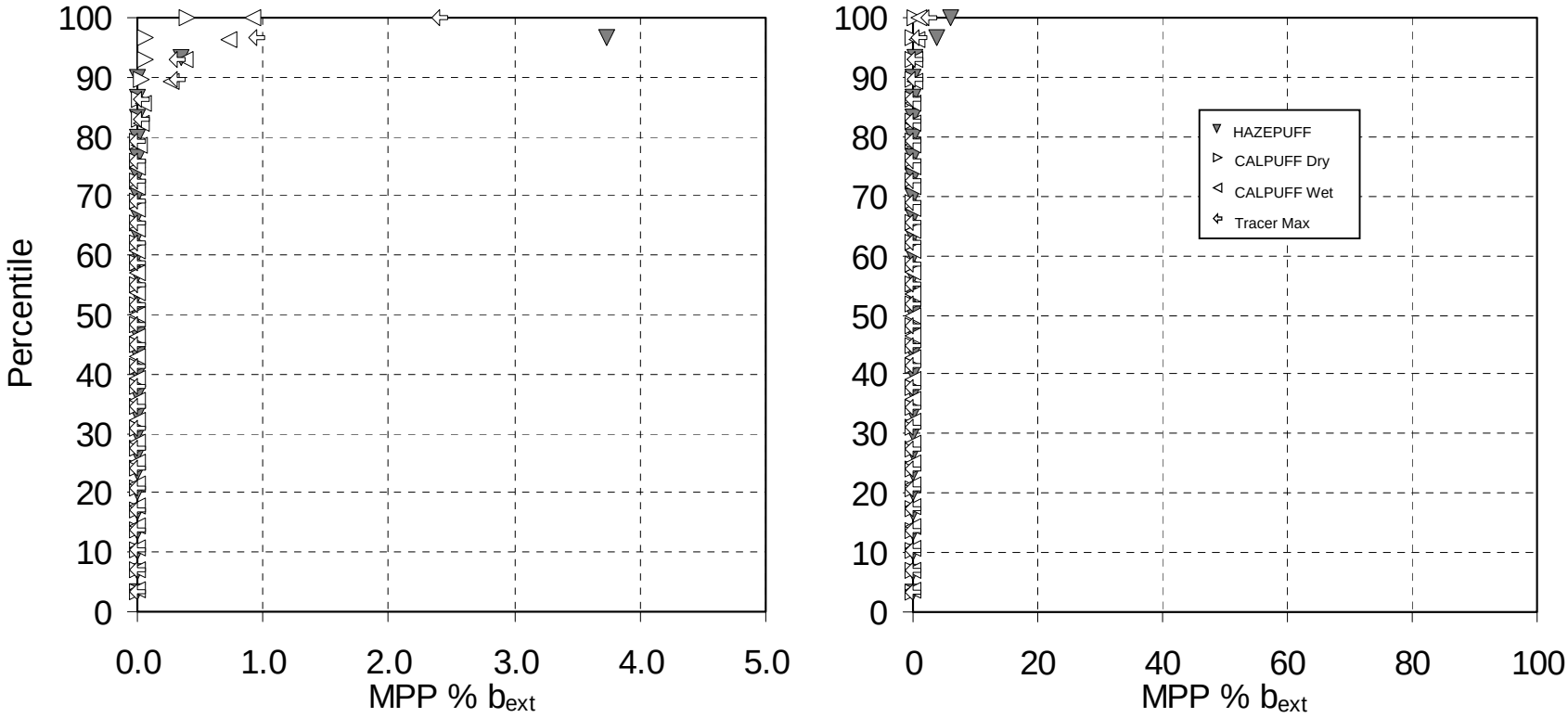


*Figure 9-19 Cumulative frequency distributions of 24-hour estimated MPP percentage contributions to measured light extinction at Meadview during the winter intensive. Filled symbols represent estimates of MPP attribution; open symbols indicate bounding calculations. Note: Inconsistent modeling results can yield similar frequency distributions.*

## 9.6 What can we say about MPP impacts on haze at GCNP during periods without tracer data?

For those periods of the year without tracer measurements, it cannot be reliably known whether MPP emissions are reaching Grand Canyon National Park. The model CALPUFF Dry was run to estimate transport and lower bound impacts during the approximately 9-month period for which radar wind profiler data was available at MPP. This data counted heavily in the calculation of the transport of emissions from MPP in the CALPUFF analysis, and thus CALPUFF was not run for periods during which wind profiler data from MPP was not available.

CALPUFF did not rely explicitly on the PFT data, but only used it for selecting the best wind field representation for the summer. For the rest of the year, when PFT data were absent, this selection was not possible and therefore the predictions may be poorer than those for the summer.

Figure 9-20 shows the frequency distribution of CALPUFF Dry predicted MPP sulfate at Meadview for the January-February, March-April, May-June, July-August, and September 1-20 periods of 1992. Predicted MPP sulfate is highest for the July-August and September periods and lowest in January-February with March-April and May-June intermediate.

Frequency distribution curves of percent of measured light extinction due to predicted MPP sulfate can be generated by applying assumed extinction efficiencies of ammonium sulfate of $2*f(RH)\ m^2g^{-1}$, as was done for the intensive study periods. These curves for the January-February, March-April, May-June, and July-August periods of 1992 are shown in Figure 9-21. A curve is not shown for the September period because ambient total light extinction data were not available for most of that period. Below about the $90^{th}$ percentile, the July-August period has the greatest predicted percent contribution of MPP sulfate to light extinction; however from about the $90^{th}$ percentile and up, the March-April period has higher predicted percent light extinction than July-August. This is a result of the higher relative humidity during the March-April period than the July-August period, causing greater predicted extinction from a given amount of sulfate.

The ratios of CALPUFF dry estimated MPP 12-hour sulfate values at Meadview for the $50^{th}$ and $90^{th}$ percentile conditions for the bi-monthly periods January-February, March-April, and May-June to the July-August period are given in Table 9-7. Corresponding light extinction ratios are given in Table 9-8.

One of the most interesting periods during the summer of 1992 was the two days following the discontinuation of tracer release from MPP at 0700 on August 31. Although visibility levels were not unusual, the first two days in September had the highest sulfate measurements recorded throughout the area that summer and represent some of the highest measurements ever made in the area. Because of the lack of tracer data, only a few methods could be used to estimate the contribution of MPP. The results of these are considered to have greater uncertainty than for periods with tracer data and are not included in the specific findings presented in this report. Some of the results of these showed relatively high MPP contribution to sulfate (Ames and Malm, 1999 – in Appendix C). However, there are alternative explanations that would indicate other sources are responsible for much of the measured sulfate (Eatough and Farber, 1999).

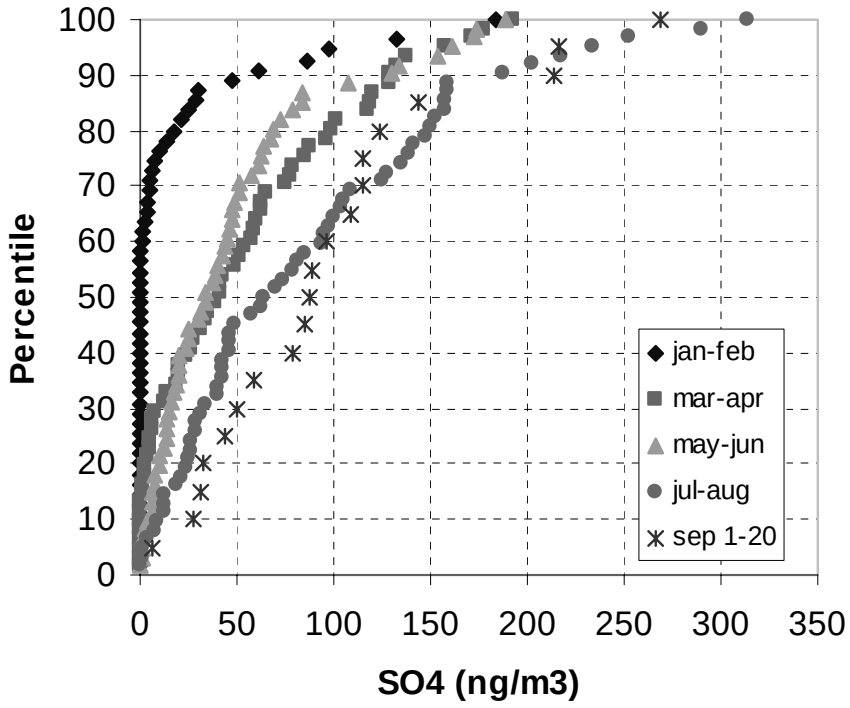


*Figure 9-20 Frequency distribution of CALPUFF Dry predicted MPP particulate sulfate at Meadview by 2 month period, 1992.*

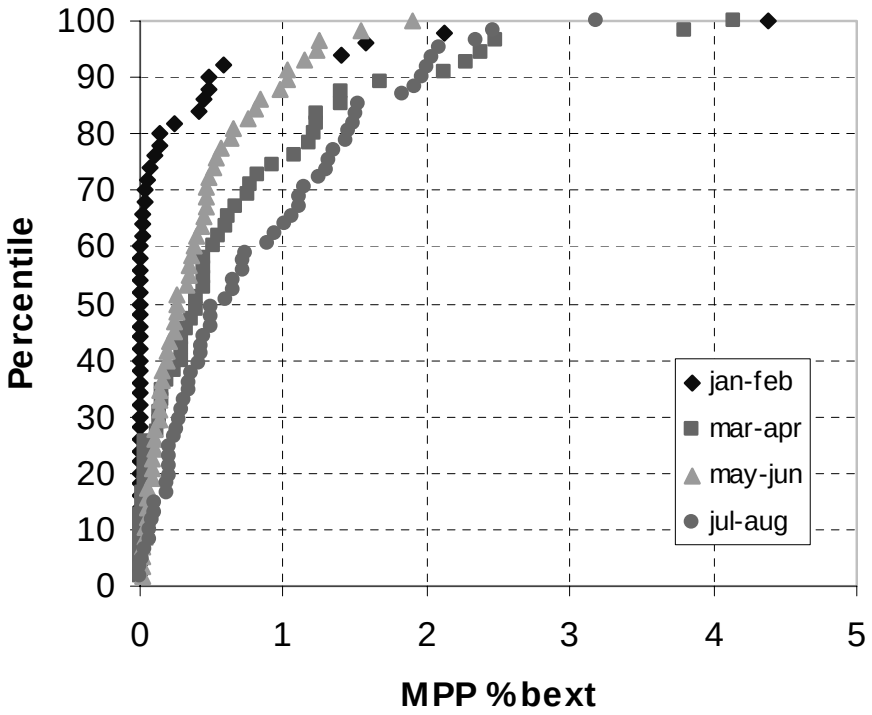


*Figure 9-21 Frequency distribution of predicted percent MPP-caused light extinction at Meadview using CALPUFF Dry, by 2 month period, 1992.*

*Table 9-7 Ratio of CALPUFF Dry estimated MPP 12-hour sulfate values for 50th and 90th percentile conditions for months not during the intensive monitoring period to corresponding values estimated for July and August.*

| January-February | | March-April | | May-June | |
|---|---|---|---|---|---|
| 50th percentile | 90th percentile | 50th percentile | 90th percentile | 50th percentile | 90th percentile |
| 0.0 | 0.2 | 0.5 | 0.8 | 0.4 | 0.6 |

*Table 9-8 Ratio of CALPUFF Dry estimated 12-hour MPP fraction of the light extinction coefficient values for 50th and 90th percentile conditions for months not during the intensive monitoring period to corresponding values estimated for July and August.*

| January-February | | March-April | | May-June | |
|---|---|---|---|---|---|
| 50th percentile | 90th percentile | 50th percentile | 90th percentile | 50th percentile | 90th percentile |
| 0.0 | 0.5 | 0.7 | 0.9 | 0.4 | 0.7 |

## 9.7 What can we infer about short-term (e.g., 3-hour) impacts on haze at GCNP?

Visibility impairment, as an instantaneous effect of air pollution, can manifest itself in much less than 12 hours. It seems unreasonable to assume that the MPP impact is uniform throughout any 12-hour sample period. Therefore the 12-and 24-hour average impact assessment results underestimate the magnitude of the peak short-term visibility impacts in any of those periods by the simple process of averaging peak impacts with low impacts. Due to inadequate information it may not be possible to properly determine the highest reasonable short-term impacts from MPP, but it should be possible to improve on the the 12- and 24-hour duration estimates.

The first question with respect to short-term impacts is what is the shortest time that would be reasonable to consider? While visibility is a short-term effect it does involve spatial averaging of the optical effects of pollutants between the viewer and the objects being viewed. Consider that a view with an object at 50 km will not be as impacted by looking through a 1km distribution of polluted air as with the same pollution concentration over the entire sight-path. Generally speaking, the average wind speed relates an air parcel's size to the time it takes to pass a fixed point. In other words a short-term peak measured at a site would be expected to be associated with a polluted air parcel with relatively small dimensions or with a larger parcel and higher wind speed. At typical wind speeds (~7 m/s) two hours corresponds to a dimension of about 50 km. Therefore the shortest time that should be considered to correspond to viewing scenic objects is an hour or two.

Estimates of MPP contribution to haze have been presented as 12-hour (7am – 7pm and 7pm – 7am) for all methods except for TAGIT which is restricted to 24-hour estimates. This was done because many of the assessment methods required tracer, particulate sulfate, $SO_2$ and/or elemental data which are only available on 12-hour (receptor sites) and 24-hour duration sampling schedule. The air quality models used for assessing MPP contributions including CALPUFF, HAZEPUFF, and ROME make short-term predictions that were averaged to 12-hours so that their results could be compared with the measurements and with the other assessment methods. Another reason for averaging to 12 and 24 hours is that in practice the shorter time period predictions of any air quality model are less comparable to measurements than the longer-term averaged predictions.

The process selected to explore short-term impacts is to develop and use a simple adjustment factor (or range of factors) to estimate the magnitude of the highest short-term impacts from the 12- and 24-hour estimated impacts. This allows adjustment to the estimates from any of the methods as presented above. Two approaches were used to develop adjustment factors. Both were only applied to the Meadview site during the summer intensive period for the MPP estimates of fractional light extinction coefficient. One approach uses the limited short-time resolution tracer data set, while the other uses CALPUFF predictions of hourly tracer concentrations. Application of the two approaches is described in Appendix B. Adjustment factors developed by the two approaches range from less than 2 to greater than 5 for adjusting the 24-hour duration estimated MPP impacts and range from less than 1.5 to 4 for adjusting the 12-hour duration estimated impacts.

From the large ranges of possible adjustment factors generated by the two approaches, it must be concluded that there is substantial uncertainty in estimates of short-term MPP contributions to light extinction coefficient at Meadview from the 12-hour and 24-hour results of the various models. This is not surprising considering the lack of data gathered specifically to address short-term impacts and the limitations of air quality models for high time resolution predictions. However, one conclusion is certain. The short-term impacts are generally greater than the long-term average estimates because every day there are periods with very little or no impact that are incorporated into the average. While the true adjustment factor probably varies from one sample period to another, it cannot be determined very well with the available methods and data. Given the range of results for the two approaches as shown above, for the purposes of this report the maximum short-term impact will be assumed to be twice the 12-hour or 24-hour impact estimates from the various methods.

### 9.8 How noticeable are the changes in haze that correspond to various fractional changes in light extinction?

Two major challenges in assessing the effects that changes in light extinction will have on perceived visual air quality are to link the optical properties of aerosols and gases to the visual appearance of the scene and to link various depictions of these changes to human perception. It is possible, with varying degrees of accuracy, to model or monitor the effect that optical properties of pollutants have on various visual parameters such as deciview, contrast, equivalent contrast, chromaticity, color difference, modulation transfer function, or just-noticeable-change (JNC). Yet it is difficult for scientists, let alone decision makers and lay persons, to "visually interpret" changes in any of these parameters that are presented in tabular or graphical form. Photography is a method that is ideally suited to present this information in a constant and reproducible form. In principle, if the ambient atmosphere was completely characterized by an intense spatial and temporal network of aerosol and optical measurements concurrent with high quality color photographs of a vista contained in the monitoring network, it should be possible to establish a data base that would show pictorially the correspondence between measured values and the appearance of the scenic resource. In reality, this approach requires an extensive, long-term monitoring program for a specific scene under a wide variety of meteorological, illumination and pollution conditions. Even then, experience has shown that the collected data usually will not be able to answer questions concerning various control or growth strategies that may be contemplated to mitigate existing visual air quality impacts or predict future visibility conditions. An alternative strategy, that was used for this project, is to collect photographs of

extremely clean periods and employ radiative transfer models and digital image processing techniques to create synthetic imagery simulating the various extinction scenarios. The process used was described in section 8.4.

Accordingly, the CD-ROM included at the end of this report provides images of vistas from Desert View and Tuweep in GCNP, each at 13 visibility levels. The baseline extinction level simulated in the images is the summertime transmissometer measured median extinction at Meadview for the Tuweep scene and at Hopi Point for the Desert View scene. In addition, visibility levels spanning from 0.5 to 1.5 times the baseline extinction level are portrayed.

To further explore the perceptibility of various changes in haze levels, the WinHaze program on the CD-ROM can be used to simulate any extinction level on several scenic vistas. For reference purposes, the median extinction measured at Meadview by the transmissometer during the summer intensive sampling period was 32.5 $Mm^{-1}$. At Hopi Point during the summer intensive sampling period, the median extinction was 35.5 $Mm^{-1}$ in the canyon and 22.7 $Mm^{-1}$ on the rim. Differences between the images are most perceptible when comparing the fine detail and color of medium and long range visual targets.

### 9.9 Level of confidence in the Project MOHAVE Findings

The findings that deal with the fractional contribution of MPP to light extinction coefficient ($F_{MPP}$) are the most applicable to the primary goal of Project MOHAVE. Those dealing with the sulfate concentration and fraction of sulfate contribution by MPP are merely the results of necessary intermediate steps in the assessment, and the computer imaging is just a tool to aid in judging the significance of the findings. The chain of reasoning needed to produce the light extinction findings can be subdivided into four basic steps: (1) MPP impact potential (same as Tracer Potential in section 8.5); (2) particulate sulfate yield from MPP emitted $SO_2$; (3) sulfate extinction efficiency; and (4) measured extinction coefficient. These are shown conceptually as the four factors on the right in Equation 9-1 and are discussed further in the text below.

$$F_{MPP} \equiv \frac{b_{SO_4,MPP}}{b_{ext}} = \frac{T\left(\frac{SO_X}{T}\right)_{MPP} \times \frac{SO_4}{SO_X} \times \frac{b_{SO_4}}{SO_4}}{b_{ext}} \qquad (9-1)$$

Though it incorporates a serious temporal resolution limitation, the ambient tracer concentration, *T*, is thought to provide a very reliable measure of the primary MPP impact at any of the monitoring sites. The uncertainty in the MPP impact potential is only a function of the tracer measurement uncertainty and the stability of the $SO_x$ to tracer ratio, $(SO_X/T)_{MPP}$, in the plume at the stack. The net effect of these factors is relatively small ($\sigma < 15\%$) at Meadview, but is larger at Hopi Point, where the tracer concentrations are smaller. Had there not been tracer data, the uncertainty for this step would be considerably larger. This can be readily appreciated by considering the much larger range of results estimated by the source contribution methods employed prior to release of the tracer data to the analysts.

Without question the largest cause of uncertainty and reason most responsible for the range of the findings among the various methods is the lack of credible information concerning the time and space variation of the yield of particulate sulfate produced from MPP. The yield can be

expressed as the ratio $SO_4/SO_x$. Much is known about the processes involved in a hypothetical sense. Dry conversion rates during daylight hours range from about 0.5% to 5% per hour with the lower end of the range more appropriate to a relatively clean desert environment. Wet conversion can be much faster but requires plume cloud interaction, is limited by the availability of oxidizing compounds, and probably stops well short of 100% conversion in any case. Finally, depositional losses of particulate sulfate and $SO_2$ between MPP and the monitoring site, especially the substantial washout that would be caused by rain events, can further change the yield.

The problem is not a lack of understanding of the processes as much as far too little information of the type needed to apply our understanding. For example, consider a day with clouds that could interact with MPP emissions. The yield could range from less than 5% to 50% or greater depending on whether the MPP emissions entirely missed or encountered clouds in a wet chemistry efficient manner. The factor of 10 range of uncertainty for sulfate yield for this example is directly translated to a factor of 10 uncertainty in the estimated MPP contribution to light extinction ($F_{MPP}$). Fortunately many days did not have a high probability for cloud interaction so the range of uncertainty is smaller. However, even under dry/cloudless conditions, the uncertainty is as much as a factor of 2 due to uncertainty in effective transport duration and number of daylight hours during transport (caused by not knowing the MPP impact timing better than the 12-hour sample period resolution). The combined range of uncertainty in yield depends on the true mixture of dry and wet conversion sample periods, which is unknown.

The method for converting the estimated MPP contributed sulfate concentration to extinction coefficient is to multiply by a relative humidity dependent extinction efficiency term (in equation 10-1, $b_{SO4}/SO_4$). The extinction efficiency term that was used was 2 $m^2/g$ times $f$(RH). The value of 2 was determined from first principle model calculations using the sulfate particle size distribution. The relative humidity function, $f$(RH), is adapted from laboratory measurements of water vapor growth data for sulfate aerosol. Sulfate particle size distribution data were available for many of the summer intensive days but not generally for other periods. The average and standard deviation of the calculations of dry particle efficiency is $2.2 \pm 0.5$ $m^2/g$, with a range from about 1.5 to 4.1 $m^2/g$. In other words there is about a 10% negative bias and roughly 25% uncertainty in the use of the rounded off value of 2 $m^2/g$. The uncertainty in the relative humidity function is smaller than the uncertainty in the dry efficiency for the relative humidity conditions experienced during all of the summer intensive period and much of the winter intensive period (RH < 90%).

The greatest confidence limit issue with respect to the extinction coefficient measurement ($b_{ext}$) is the possibility of a positive bias in the transmissometer measurements for Meadview during the summer intensive (discussed further in Section 5). To assess the magnitude of the effects of this possible bias on the findings concerning the MPP contributions to light extinction coefficient, particle calculated light extinction coefficient values were used in a separate calculation of the findings (Figure 9-6and Meadview during the summer where the range is larger by about one third to one half using the calculated values.

Table 9-5). The calculated extinction coefficients are more likely to underestimate the true light extinction coefficient than to overestimate it. Using the calculated extinction increased the 90$^{th}$ percentile values at Meadview during the summer by about one third to one half. The random

measurement error for the transmissometer determined light extinction coefficient is about 10% to 15%.

As indicated above, most of the uncertainty in the principal findings of Project MOHAVE is the result of uncertainty in the yield of particulate sulfate from $SO_2$. The various methods used to estimate the contribution of MPP to visibility at GCNP used a number of approaches from simplistic assumptions to sophisticated meteorological/chemical modeling to attempt to assign the reasonable values and constructive limits (e.g. CALPUFF Dry and Wet). For this report, the ranges of estimate by the various methods at different points in the cumulative frequency distribution are taken as credible ranges for the findings. To examine the plausibility of this approach in light of the uncertainty in the yield, a reconfiguration of the data using the most reliable steps in the process was conducted by solving Equation 9-1 for the yield, $(SO_4/SO_X)$.

Figure 9-22 and Figure 9-23 show time plots of the yield for each 12-hour period that would be required to generate 1% and 10% of the measured light extinction coefficient in summer at the Meadview and Hopi Point sites (i.e. set $F_{MPP}$ = 1% and $F_{MPP}$ = 10%). This information was produced solely from the tracer measurements ($T$) along with the emissions ratio of $SO_x$ to tracer ratio ($SO_x/T$) for MPP, the extinction efficiency ($b_{SO4}/SO_4$) and measured extinction coefficient ($b_{ext}$) as described above. Obviously, a yield greater than 100% is not possible, so any point above 100% yield (horizontal line) is a 12-hour period where MPP could not have contributed 1% or 10% of the light extinction coefficient. While an attainable upper limit is not generally agreed upon, most of the analysts would consider 50% a pretty large fraction even for wet conversion over the distances involved here and 5% to 10% might be considered easily attainable with dry conversion for transport during daylight hours.

These time plots illustrate the potential for MPP to contribute at the 1% and 10% of the light extinction coefficient levels during the summer intensive period. Using any reasonable upper limit (e.g., between 50% and 100%) as a yield criterion, one would say that most of the time MPP doesn't have the potential to contribute as much as 10% of the light extinction coefficient at Meadview and as much as 1% of the light extinction coefficient at Hopi Point. Using any reasonable lower limit as a yield criterion (e.g. between 5% and 10% for daytime transport), one would say that MPP often has the potential to contribute at least 1% of the light extinction coefficient at Meadview.

Yield is the big unknown in the process. However, these time plots demonstrate that the use of any user-selected reasonable limits for conversion generates results that are broadly consistent with the ranges that are the findings shown in Section 9.6. This assessment can not shed any light on which of the methods is more likely to be correct overall or during any particular time period, but it does show that the true values are unlikely to lie outside of the ranges.

Uncertainty necessarily increases for the findings concerning MPP contributions during non-tracer periods. CALPUFF predictions of tracer concentration at Meadview for the period with the augmented upper air wind data are the basis for the assessment of the non-tracer period MPP contributions. CALPUFF tracer estimates are arguably as good at predicting measured tracer as those of any of the other air quality models. There is no way to know whether the agreement would be as good or worse for the periods without tracer and so the result that 'March and April

may have comparable MPP contributions to those found during the summer intensive period' should be treated as semi-quantitative at best.

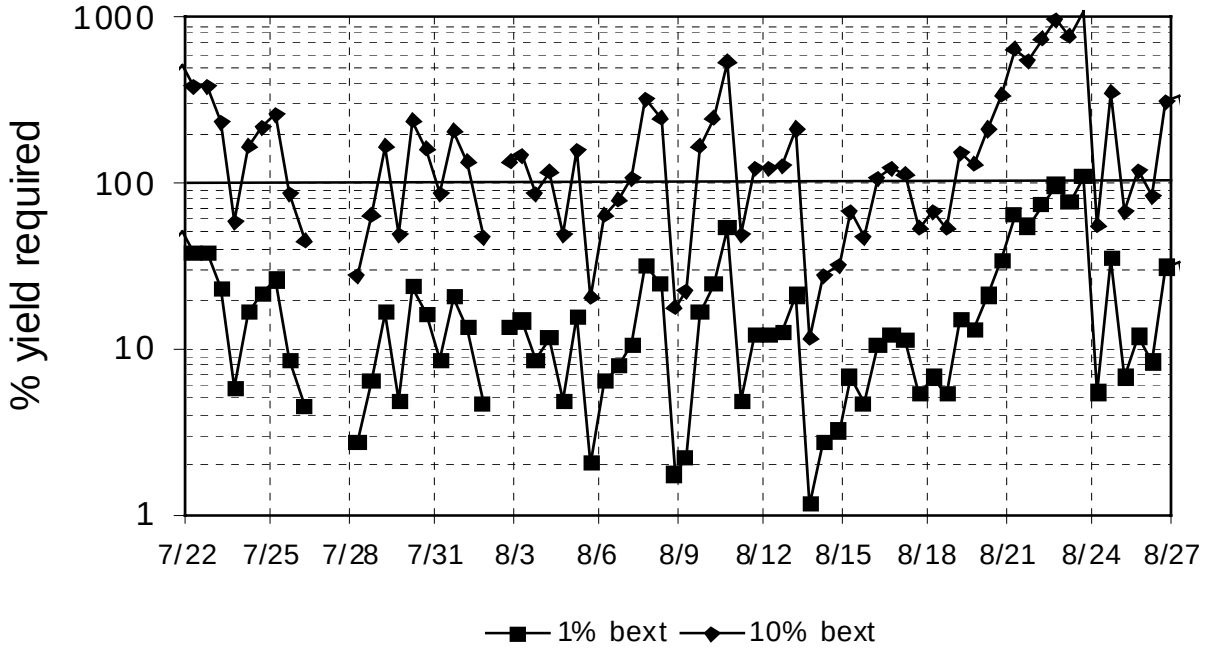


*Figure 9-22: Time plots of the particulate sulfate yield for each 12-hour period that would be required to generate 1% and 10% of the measured light extinction coefficient in summer at Meadview.*

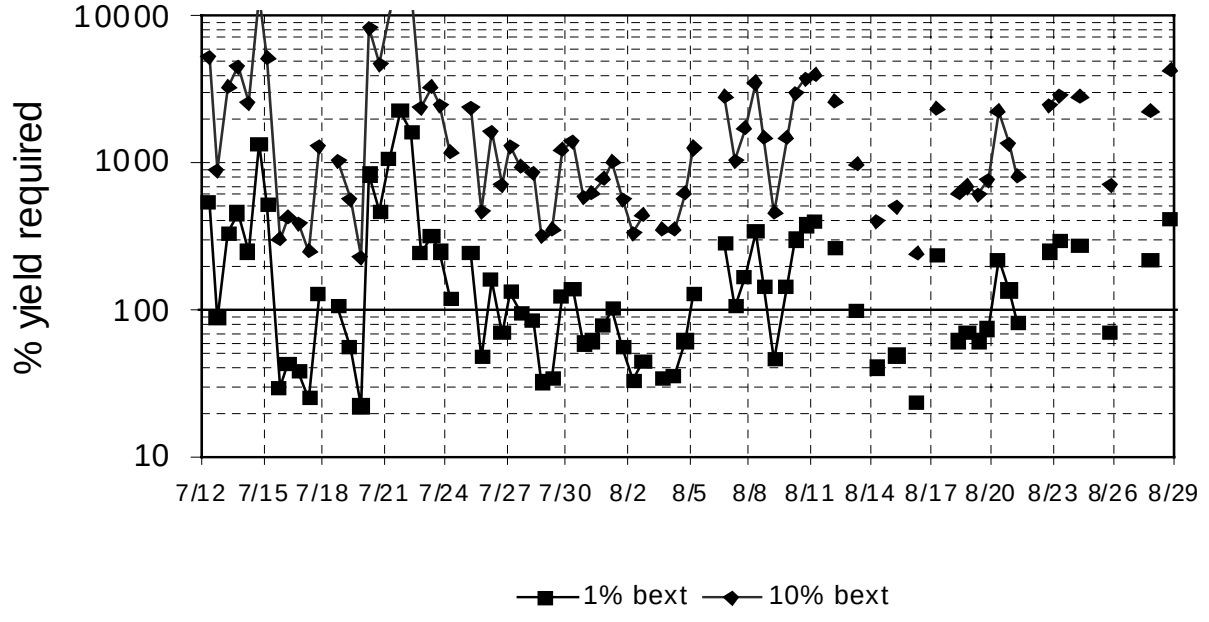


*Figure 9-23 Time plots of the particulate sulfate yield for each 12-hour period that would be required to generate 1% and 10% of the measured light extinction coefficient in summer at Hopi Point.*

Uncertainty in the adjustment factor to estimate the maximum MPP short-term impacts for any 12-and 24-hour estimate contribution to light extinction coefficient may be best expressed by the ranges of results of the two methods that generated the consensus factor. For the factor to adjust from the 12-hour estimates the range was about 1.5 to 4 and for the factor to adjust from 24-hour estimates the range was about 2 to 8. The consensus value of 2 is near the low end of the range principally because of the concern that this term may be more used to adjust the highest MPP impact estimates which may have involved longer than average impacts. Certainly if the consensus adjustment term were used to adjust all of the 12- or 24-hour predictions the results would be biased too low. However, it was never the intent of the data analysts to use this adjustment so broadly. It was developed solely to give a semi-quantitative sense of how much greater the short-term impact may be than the sample period averaged impacts.

It is useful to view the computer simulated photographs in the CD-ROM accompanying this report when considering whether the ranges of estimated MPP fractional contribution to light extinction coefficient are sufficiently narrow to make judgments concerning MPP impacts. Take for example the $90^{th}$ percentile range for Meadview summer as shown in Table 9-4 with a range from 1.3% to 5.0%. While the range is a factor of four, it seems unlikely that the difference in these two estimates would be visible. Even if the values were multiplied by 2 to crudely estimate the maximum short-term impacts the differences would be less than 10%.